
Extrapolation and Spectral Bias of Neural Nets with Hadamard Product: a Polynomial Net Study

Yongtao Wu, Zhenyu Zhu, Fanghui Liu, Grigorios G Chrysos, Volkan Cevher

EPFL, Switzerland

{[first name].[surname]}@epfl.ch

Abstract

Neural tangent kernel (NTK) is a powerful tool to analyze training dynamics of neural networks and their generalization bounds. The study on NTK has been devoted to typical neural network architectures, but it is incomplete for neural networks with Hadamard products (NNs-Hp), e.g., StyleGAN and polynomial neural networks (PNNs). In this work, we derive the finite-width NTK formulation for a special class of NNs-Hp, i.e., polynomial neural networks. We prove their equivalence to the kernel regression predictor with the associated NTK, which expands the application scope of NTK. Based on our results, we elucidate the separation of PNNs over standard neural networks with respect to extrapolation and spectral bias. Our two key insights are that when compared to standard neural networks, PNNs can fit more complicated functions in the extrapolation regime and admit a slower eigenvalue decay of the respective NTK, leading to a faster learning towards high-frequency functions. Besides, our theoretical results can be extended to other types of NNs-Hp, which expand the scope of our work. Our empirical results validate the separations in broader classes of NNs-Hp, which provide a good justification for a deeper understanding of neural architectures.

1 Introduction

In deep learning theory, neural tangent kernel (NTK) [Jacot et al., 2018] is a powerful analysis tool that links the training dynamics of neural networks (NNs) trained by gradient descent to kernel regression [Jacot et al., 2018, Arora et al., 2019]. NTK provides a tractable analysis for several phenomena in deep learning, e.g., the global convergence of gradient descent [Chizat et al., 2019, Du et al., 2019a,c], the inductive bias behind NNs [Bietti and Mairal, 2019], the spectral bias toward different frequency components [Cao et al., 2019, Choraria et al., 2022], the extrapolation behavior [Xu et al., 2021], and the generalization ability [Huang et al., 2020]. The study on the NTK has been devoted to typical NNs architectures, e.g., fully-connected NNs [Jacot et al., 2018], residual NNs [Tirer et al., 2020, Huang et al., 2020], convolutional NNs [Arora et al., 2019], graph NNs [Du et al., 2019b] and recurrent NNs [Alemohammad et al., 2021].

Recently, NNs with Hadamard products (NNs-Hp), e.g., StyleGAN [Karras et al., 2019], polynomial neural networks [Chrysos et al., 2020], non-local multiplicative networks [Babiloni et al., 2021], have received increasing attention due to their expressivity and efficiency over traditional NNs [Chrysos et al., 2021a, Campbell and Broun, 2000, Su et al., 2020]. There have been several works attempting to demystify the success of NNs-Hp. For instance, Fan et al. [2021] prove that second-degree multiplicative interactions allow NNs-Hp to enlarge the set of functions that can be represented exactly with zero error. Choraria et al. [2022] reveal that NNs-Hp with second-degree multiplicative interactions yield a faster learning of high-frequency function during training in the NTK regime. Yet, the theoretical analysis of NNs-Hp with high-degree multiplicative interactions is still unclear. More importantly, when using NTK for analysis, only deriving the NTK matrix is not enough. The

complete and rigorous proof is achieved by including the stability of empirical NTK during training and the equivalence to kernel regression. This is crucial to allow for NTK-based analysis of typical NNs [Arora et al., 2019, Tirer et al., 2020] but is still missing for NNs-Hp.

Polynomial neural networks (PNNs) [Chrysos et al., 2021a], a special class of NNs-Hp [Jayakumar et al., 2020], have showcased remarkable performance on a broad range of applications. As a step for analyzing NNs-Hp, in this work, we take PNNs as an example, derive the NTK for PNNs with high-degree multiplicative interactions and present a rigorous proof for the equivalence to the kernel regression predictor. This analysis enables us to further examine properties of PNNs in a theoretical perspective, e.g., the extrapolation [Haley and Soloway, 1992, Barnard and Wessels, 1992, Xu et al., 2021]. Neural networks have demonstrated a stellar in-distribution performance but admit some weaknesses in extrapolating simple arithmetic problems [Saxton et al., 2019] or learning simple functions [Haley and Soloway, 1992, Sahoo et al., 2018]. Recently, Xu et al. [2021] theoretically and empirically point out that two-layer fully-connected NNs with ReLU can only extrapolate to linear functions. The contrast on the in-/out of-distribution performance of standard NNs motivates us to scrutinize the extrapolation performance of PNNs. Additionally, studying the NTK of PNNs also allows us to investigate its spectral bias.

Overall, our main contributions and findings can be summarized as follows:

- We derive the NTK formulation for PNNs with high-degree multiplicative interactions, and give a concrete bound of the widths requirement for convergence to the NTK at initialization, and stability during training, which allows us to bridge the gap among PNNs trained via gradient descent and kernel regression predictor.
- We provably demonstrate the extrapolation behavior of PNNs as well as other NNs-Hp, including multiplicative filter networks and non-local multiplicative networks. Our findings highlight that PNNs can extrapolate to unseen data in a non-linear way. Besides, the spectral analysis of NTK of PNNs is also given for better understanding. PNNs admit a slower eigenvalue decay when compared to standard NNs, which leads to a faster learning towards high-frequency functions.
- We empirically show the advantage of NNs-Hp over standard NNs in learning commonly used functions, performing arithmetic extrapolation in real-world dataset, and conducting visual analogy extrapolation task. We scrutinize the role of multiplicative interactions in the task of learning spherical harmonics.

2 Background

In this section, we establish the notation, provide an overview of the NTK, and summarize the most closely related work in NNs-Hp as well as extrapolation.

2.1 Notation

The core operators and symbols are summarized in Table 2 at Appendix A. Vectors (matrices) are symbolized by lowercase (uppercase) boldface letters, e.g., \mathbf{a} , \mathbf{A} . We use the shorthand $[n] := \{1, 2, \dots, n\}$ for a positive integer n . We use $\{\mathbf{x}_i\}_{i=1}^{|\mathcal{X}|}$ and $\{y_i\}_{i=1}^{|\mathcal{X}|}$ to present the input features and their labels of the training set $(\mathcal{X}, \mathcal{Y})$ in a compact space, where $|\mathcal{X}|$ denotes the cardinality. We symbolize by $K(\mathbf{x}, \mathbf{x}')$ the neural tangent kernel with respect to input \mathbf{x} and \mathbf{x}' , the kernel matrix $\mathbf{K} \in \mathbb{R}^{|\mathcal{X}| \times |\mathcal{X}|}$ with $K^{(ij)} = K(\mathbf{x}_i, \mathbf{x}_j)$. Next, we denote by $\boldsymbol{\theta}_t$ the parameter vector, $\ell_2(\boldsymbol{\theta}_t)$ the empirical training loss, and $\hat{\mathbf{K}}_t$ the empirical NTK Gram matrix at time step t . The following notation is used:

$$\ell_2(\boldsymbol{\theta}_t) = \frac{1}{2} \sum_{(\mathbf{x}_i, y_i) \in (\mathcal{X}, \mathcal{Y})} (f(\mathbf{x}_i; \boldsymbol{\theta}_t) - y_i)^2, \quad f(\boldsymbol{\theta}_t) = \text{vec}(\{f(\mathbf{x}_i; \boldsymbol{\theta}_t)\}_{\mathbf{x}_i \in \mathcal{X}}) \in \mathbb{R}^{|\mathcal{X}|},$$

$$J(\boldsymbol{\theta}_t) = \frac{\partial f(\boldsymbol{\theta}_t)}{\partial \boldsymbol{\theta}} \in \mathbb{R}^{|\mathcal{X}| \times |\boldsymbol{\theta}|}, \quad \hat{\mathbf{K}}_t = J(\boldsymbol{\theta}_t)J(\boldsymbol{\theta}_t)^\top \in \mathbb{R}^{|\mathcal{X}| \times |\mathcal{X}|}.$$

2.2 Neural tangent kernel

Neural networks (NNs) are relevant to the kernel method, under proper initialization [Daniely et al., 2016, de G. Matthews et al., 2018]. Jacot et al. [2018] provably demonstrate the equivalence between the training dynamics by gradient descent and kernel regression induced by NTK when employing the ℓ_2 loss. Below, we recall the exact formula regarding the NTK of N -layer ($N > 2$) fully-connected NNs with ReLU activation functions σ . The corresponding NTK $K(\mathbf{x}, \mathbf{x}') = K_N(\mathbf{x}, \mathbf{x}')$ could be computed recursively by:

$$K_0(\mathbf{x}, \mathbf{x}') = \Sigma_0(\mathbf{x}, \mathbf{x}') = \mathbf{x}^\top \mathbf{x}', \quad K_n(\mathbf{x}, \mathbf{x}') = \Sigma_n(\mathbf{x}, \mathbf{x}') + 2K_{n-1}(\mathbf{x}, \mathbf{x}') \cdot \dot{\Sigma}_n(\mathbf{x}, \mathbf{x}'),$$

$\forall n \in [N]$, where the covariance Σ_n and its derivative $\dot{\Sigma}_n$ are defined as:

$$\Sigma_n(\mathbf{x}, \mathbf{x}') = 2\mathbb{E}_{(u,v) \sim \mathcal{N}(0, \Lambda_n)}[\sigma(u)\sigma(v)], \quad \dot{\Sigma}_n(\mathbf{x}, \mathbf{x}') = \mathbb{E}_{(u,v) \sim \mathcal{N}(0, \Lambda_n)}[\sigma'(u)\sigma'(v)]$$

$$\Lambda_n = \begin{pmatrix} \Sigma_{n-1}(\mathbf{x}, \mathbf{x}) & \Sigma_{n-1}(\mathbf{x}, \mathbf{x}') \\ \Sigma_{n-1}(\mathbf{x}, \mathbf{x}') & \Sigma_{n-1}(\mathbf{x}', \mathbf{x}') \end{pmatrix}, \forall n \in [N].$$

Furthermore, the aforementioned NTK is extended to residual NNs [Tirer et al., 2020, Huang et al., 2020], convolutional NNs [Arora et al., 2019], graph NNs [Du et al., 2019b], and recurrent NNs [Alemohammad et al., 2021]. One of the roles of such kernel is to analyze the training behavior of the neural network in the over-parameterization regime [Allen-Zhu et al., 2019, Chizat et al., 2019, Du et al., 2019a,c, Zou et al., 2020]. For instance, Lee et al. [2019] showcase that NNs under the NTK parameterization trained via gradient descent of any depth evolve to linear models. Meanwhile, the inductive bias of convolutional networks, e.g., deformation stability of the images, has been studied in the NTK regime [Bietti and Mairal, 2019].

2.3 Neural networks with Hadamard product

The ideas of augmenting NNs with Hadamard products to allow multiplicative interactions can be traced back to at least [Ivakhnenko, 1971] that investigate the learnable polynomial relationships. Most of the early work e.g., Group Method of Data Handling [Ivakhnenko, 1971], pi-sigma network [Shin and Ghosh, 1991] do not scale well for high-dimensional signals. Chrysos et al. [2021b] factorize the weight of NNs-Hp based on tensor decompositions to reduce the number of parameters. They exhibit how to convert popular networks, such as residual networks, and convolutional NNs to the form of NNs-Hp. StyleGAN can be also considered as a special type of NNs-Hp [Chrysos et al., 2019]. New efforts have recently emerged to improve the architecture of the network with Hadamard products [Chrysos et al., 2022, Babiloni et al., 2021, Chrysos et al., 2021a]. In this work, we adopt the complementary approach and focus on the extrapolation as well as the spectral bias from a theoretical perspective.

2.4 Extrapolation

The study of extrapolation properties of NNs dates at least back to the 90's [Barnard and Wessels, 1992, Kramer and Leonard, 1990]. Experimental results show poor performance of NNs in case of learning simple functions [Barnard and Wessels, 1992]. Browne [2002] also suggest that fully-connected NNs cannot extrapolate well and then illustrate how the representation of the input impact the extrapolation. Xu et al. [2021] provably present the extrapolation behavior of fully-connected NNs and Graph neural networks. Specifically, they show that two-layer fully-connected NNs with ReLU activation function extrapolate to linear function in extrapolation region. Our work exhibits that NNs-Hp can learn high degree nonlinear function. Apart from fully-connected NNs, Martius and Lampert [2016], Sahoo et al. [2018] showcase a novel family of functions with linear mapping and a non-linear transformation, which allows to use sine and cosine as nonlinearities, enabling such networks to learn well in analytical expressions. Note that there exist multiplication units in EQL, which is similar to the multiplicative interactions in NNs-Hp. Lastly, extrapolation is often considered in the context of out-of-distribution (OOD). There are other types of OOD problems with specific setting among machine learning community [Shen et al., 2021]. Domain adaption assumes the source and the target domains lie in the same feature space but with different distributions [Kouw and Loog, 2019], which differs from extrapolation. Another category of methodologies to solve the OOD generalization problem, called invariant learning, aims to discover high-level invariance feature from low-level observations through latent causal mechanisms [Arjovsky et al., 2019, Rosenfeld et al., 2021]. We believe our analysis can also encourage the usage of NNs-Hp in these OOD problems.

3 Analysis of polynomial neural networks

Our analysis admits the following structure: we firstly study the NTK of PNNs in Section 3.1, which allows us to conduct analysis towards extrapolation in Section 3.2, and spectral bias in Section 3.3. In Appendix F and G, of the supplementary, we consider extensions beyond PNNs to other families of NNs-Hp, e.g. multiplicative filter networks and non-local networks with Hadamard product.

3.1 Neural tangent kernel

We now derive the NTK for PNNs, then we bridge the gap between the PNNs trained by gradient descent with respect to squared loss and the kernel regression predictor involving the NTK. The goal of such networks is to learn an N -degree ($N \geq 2$) polynomial expansion that outputs $f(\mathbf{x}) \in \mathbb{R}$ with respect to the input $\mathbf{x} \in \mathbb{R}^d$. For simplifying the proof, we consider the following formulation, which is a reparameterization version of PNNs [Zhu et al., 2022]. The output is given by:

$$\mathbf{y}_1 = \sqrt{\frac{2}{m}}\sigma(\mathbf{W}_1\mathbf{x}), \quad f(\mathbf{x}) = \sqrt{\frac{2}{m}}(\mathbf{W}_{N+1}\mathbf{y}_N), \quad \mathbf{y}_n = \sqrt{\frac{2}{m}}\sigma(\mathbf{W}_n\mathbf{x}) * \mathbf{y}_{n-1}, \quad n = 2, \dots, N, \quad (1)$$

where σ is the ReLU activation function, each element in $\mathbf{W}_{N+1} \in \mathbb{R}^{1 \times m}$ and $\mathbf{W}_n \in \mathbb{R}^{m \times d}$, $\forall n \in [N]$ is independently sampled from $\mathcal{N}(0, 1)$. Three remarks are in place: a) We multiply by the scaling factor $\sqrt{\frac{2}{m}}$ after each degree to ensure that the norm of the network output is preserved at initialization with infinite-width setting. b) ReLU is usually required to increase the performance of NNs-Hp in experiments [Chrysos et al., 2021b]. c) The original formulation before reparameterization that is used in practice can be founded in Appendix A.1.

Theorem 1. *The NTK of N -degree PNNs, denoted by $K(\mathbf{x}, \mathbf{x}')$, can be derived as:*

$$K(\mathbf{x}, \mathbf{x}') = 2N \cdot \langle \mathbf{x}, \mathbf{x}' \rangle \kappa_1(\mathbf{x}, \mathbf{x}') (\kappa_2(\mathbf{x}, \mathbf{x}'))^{N-1} + 2(\kappa_2(\mathbf{x}, \mathbf{x}'))^N, \quad (2)$$

where κ_1 and κ_2 are defined by taking the random Gaussian vector $\mathbf{w} \in \mathbb{R}^d$

$$\kappa_1 = \mathbb{E}_{\mathbf{w} \sim \mathcal{N}(\mathbf{0}, \sqrt{\frac{2}{m}} \cdot \mathbf{I})} (\dot{\sigma}(\mathbf{w}^\top \mathbf{x}) \cdot \dot{\sigma}(\mathbf{w}^\top \mathbf{x}')), \quad \kappa_2 = \mathbb{E}_{\mathbf{w} \sim \mathcal{N}(\mathbf{0}, \sqrt{\frac{2}{m}} \cdot \mathbf{I})} (\sigma(\mathbf{w}^\top \mathbf{x}) \cdot \sigma(\mathbf{w}^\top \mathbf{x}')). \quad (3)$$

The proof, which is provided in Appendix B.1, is based on the standard NTK calculations. Differently from the NTK of fully-connected NNs, the existence of multiplicative interaction in PNNs induces the product form of multiple kernels.

Next, we provide the following theorem that gives a concrete requirement for the width of the networks that is sufficient for nonasymptotic convergence to the NTK at initialization,

Theorem 2. *(Convergence to the NTK). Consider N -degree PNNs, and assume that the width $m \geq 2^{4N-2} \log^{2N-1}(2N/\delta)$ for any $\delta \in (0, 1)$, then given two inputs \mathbf{x}, \mathbf{x}' on the unit sphere, with probability at least $1 - \delta$ over the randomness of initialization, we have that*

$$|\langle \nabla f(\mathbf{x}), \nabla f(\mathbf{x}') \rangle - K(\mathbf{x}, \mathbf{x}')| \leq 4N\rho e \sqrt{\frac{\log(2N/\delta)}{m}},$$

$$\text{where } \rho = \sqrt{2}^{2N-1} \sqrt{8} e^3 (2\pi)^{1/4} e^{1/24} (e^{2/e} (2N-1)/2)^{(2N-1)/2}.$$

Remark: This result exhibits that the inner product of the Jacobian converges to the NTK at initialization, which has not been studied before for PNNs. This theorem allows us to further analyze the extrapolation of networks from the perspective of the NTK. It should be noted that the term ρ and the width are exponential with respect to the degree N , but the degree N is not large in practice, e.g., at most 15 in Chrysos et al. [2021a]. Hence the bound is fair and reasonable.

The technical key issue of the proof is to provide probability estimates for the multiplication of several sub-exponential random variables. To this end, we rely on the concentration of sub-Weibull random variables [Zhang and Chen, 2020] to complete the proof, which is deferred to Appendix B.2.

Below, we show that under certain conditions, the limiting NTK of PNNs stays constant when training with gradient descent using the squared loss.

Theorem 3 (Stability of the NTK during training). *Given PNNs in Eq. (1), assume $\lambda_{\min}(\mathbf{K}) > 0$ and the training data $(\mathcal{X}, \mathcal{Y})$ in a compact space admitting $\mathbf{x} \neq \tilde{\mathbf{x}}$ for all $\mathbf{x}, \tilde{\mathbf{x}} \in \mathcal{X}$, then there exist some constants $R_0 > 0$, $M > 1$, and $Q > 1$ such that for every $m > M$, when minimizing the squared loss with gradient descent and sufficient small learning rate $\eta_0 < 2(\lambda_{\min}(\mathbf{K}) + \lambda_{\max}(\mathbf{K}))^{-1}$, the following inequality holds with high probability over the random initialization of model parameters:*

$$\sup_t \|\hat{\mathbf{K}}_t - \hat{\mathbf{K}}_0\|_F \leq \frac{6Q^3 R_0}{\lambda_{\min}(\mathbf{K})\sqrt{m}}. \quad (4)$$

Remark: Eq. (4) shows that $\hat{\mathbf{K}}_t \xrightarrow{m \rightarrow \infty} \hat{\mathbf{K}}_0$. Combining this with Theorem 2 that states $\hat{\mathbf{K}}_0 \xrightarrow{m \rightarrow \infty} \mathbf{K}$, we have $\hat{\mathbf{K}}_t \xrightarrow{m \rightarrow \infty} \mathbf{K}$. Thus, the equivalence to the kernel regression is established. Note that Theorem 3 is an extension from the corresponding theorem of NNs with residual connection [Tirer et al., 2020] to PNNs. This property allows us to characterize the training process as kernel regression.

Regarding the proof of Theorem 3, we firstly introduce the norm control of the Gaussian weight matrices and then derive the local boundness and local Lipschitzness. The last step is to apply the induction rules over different time steps. Details are presented in the Appendix B.3.

3.2 Extrapolation behavior

Firstly, we provide the definition of extrapolation from Xu et al. [2021] as follows.

Definition 1. Extrapolation occurs when the domain of test samples is larger than the support of the training distribution.

Remark: The definition presented above is different from the one in Balestrieri et al. [2021] that claims extrapolation occurs when the test samples fall outside of the convex hull of the training set. Even though these definitions are not completely compatible, both definitions are suitable for our subsequent analysis.

The derived kernel in the previous section enables us to study how PNNs with ReLU activation trained by gradient descent extrapolates. Note that our theorem can also be extended to the raw PNNs without activation function.

Theorem 4 (γ -degree extrapolation of N -degree PNNs). *Suppose we train N -degree ($N \geq 2$) PNNs $f : \mathbb{R}^d \rightarrow \mathbb{R}$ with infinite-width on $\{(\mathbf{x}_i, y_i)\}_{i=1}^{|\mathcal{X}|}$, and the network is optimized with the squared loss in the NTK regime. For any direction $\mathbf{v} \in \mathbb{R}^d$ that satisfies $\|\mathbf{v}\|_2 = \max\{\|\mathbf{x}_i\|_2\}$, let $\mathbf{x}_0 = t\mathbf{v}$ and $\mathbf{x} = \mathbf{x}_0 + h\mathbf{v}$ with $t > 1$ and $h > 0$ be the extrapolation data points, the output $f(\mathbf{x}_0 + h\mathbf{v})$ follows a γ -degree ($\gamma \leq N$) function with respect to h .*

Apart from PNNs, we also consummate Xu et al. [2021] that consider the extrapolation of fully-connected NNs with only two-layer. We provide the following generalized theorem for N -layer ($N > 2$) fully-connected NNs.

Theorem 5 (Linear extrapolation of N -layer fully-connected NNs). *Suppose we train N -layer ($N \geq 2$) fully-connected NNs $f : \mathbb{R}^d \rightarrow \mathbb{R}$ on $\{(\mathbf{x}_i, y_i)\}_{i=1}^{|\mathcal{X}|}$. For any direction $\mathbf{v} \in \mathbb{R}^d$ that satisfies $\|\mathbf{v}\|_2 = \max\{\|\mathbf{x}_i\|_2\}$, $\mathbf{x}_0 = t\mathbf{v}$ and $\mathbf{x} = \mathbf{x}_0 + h\mathbf{v}$ with $t > 1$ and $h > 0$ are extrapolation data points, the output $f(\mathbf{x}_0 + h\mathbf{v})$ follows a linear function with respect to h .*

We have already shown that PNNs extrapolate to a function with specific degree and are more flexible than fully-connected NNs. However, only knowing the information of the degree of the extrapolation function is not enough. Naturally, we might ask under which condition PNNs can achieve successful extrapolation. Below, we build our analysis in the NTK regime and show how the geometry of the training set affects the behavior of PNNs.

Theorem 6 (Condition for exact extrapolation of PNNs). *Let $f_\rho(\mathbf{x}) = \mathbf{x}^\top \boldsymbol{\beta} \mathbf{x}$ be the target function with $\mathbf{x} \in \mathbb{R}^d$ and $\boldsymbol{\beta} \in \mathbb{R}^{d \times d}$. Suppose that $\{\mathbf{x}_i\}_{i=1}^{|\mathcal{X}|}$ contains the orthogonal basis $\{\mathbf{e}_i\}_{i=1}^d$ and $\{-\mathbf{e}_i\}_{i=1}^d$. Then if we train two-degree PNNs f on $\{(\mathbf{x}_i, f_\rho(\mathbf{x}_i))\}_{i=1}^{|\mathcal{X}|}$ with the squared loss in the NTK regime, we have $f(\mathbf{x}) = \mathbf{x}^\top \boldsymbol{\beta} \mathbf{x}$ for all $\mathbf{x} \in \mathbb{R}^d$.*

Remark: This result only considers quadratic functions as our proof heavily relies on the construction of the feature map of the NTK, which is harder for the high-degree case.

Due to constrained space, the proof of aforementioned theorems can be found in Appendix C.1 to C.3.

3.3 Spectral analysis

In this section, we characterize the approximation properties of N -degree PNNs in the in-distribution regime. By studying the spectral analysis in the form of a Mercer decomposition, we explicitly show the eigenvalues and eigenfunctions of NTK. We firstly introduce some notation. Denote by $\{Y_{k,j}\}_{j=1}^{N(d,k)}$ the spherical harmonics of degree k in $d + 1$ variables. $G_k^{(\gamma)}$ represents the Gegenbauer polynomials with respect to the weight function $x \mapsto (1 - x^2)^{\gamma - \frac{1}{2}}$ and degree k . Finally, denote by $F(d, k) := \frac{2k+d-1}{k} \binom{k+d-2}{d-1}$.

The following lemma enables us to connect spherical harmonics to Gegenbauer polynomials.

Lemma 1. [Frye and Efthimiou, 2012, Theorem 4.11] *For any $\mathbf{x}, \mathbf{x}' \in \mathbb{S}^d$, the k -degree spherical harmonics in $d + 1$ variables satisfies:*

$$\sum_{j=1}^{F(d,k)} Y_{k,j}(\mathbf{x})Y_{k,j}(\mathbf{x}') = F(d, k)G_k^{(\frac{d-1}{2})}(\langle \mathbf{x}, \mathbf{x}' \rangle).$$

For any dot product Mercer kernel K' , denote by $(\mu_k)_{k=0}^{\infty}$ the eigenvalues associated to the kernel, we can apply the following Mercer's decomposition in the form of spherical harmonics, and using Lemma 1 we obtain:

$$K'(\mathbf{x}, \mathbf{x}') = \sum_{k=0}^{\infty} \mu_k \sum_{j=1}^{F(d,k)} Y_{k,j}(\mathbf{x})Y_{k,j}(\mathbf{x}') = \sum_{k=0}^{\infty} \mu_k F(d, k)G_k^{(\frac{d-1}{2})}(\langle \mathbf{x}, \mathbf{x}' \rangle), \quad (5)$$

In order to study the decay rate of the eigenvalues, we can express the NTK as the product of multiple kernels and present the decay rate of the eigenvalues of PNNs.

Theorem 7. *Consider PNNs with N -degree ($N \geq 2$) multiplicative interactions and denote by $(\mu_k)_{k=0}^{\infty}$ the eigenvalues associated to the NTK. Then for $k \gg d$, we have $\mu_k = \Omega((N^2k)^{-d/2})$.*

The proof can be found in Appendix D. As a comparison, the decay rate for both deep fully-connected NNs and residual NNs is $\Omega((k)^{-d})$ [Belfer et al., 2021]. Thus, we can see a slower decay rate when inserting Hadamard product into standard NNs, which leads to a faster learning towards high-frequency functions.

4 Experiments

Our experiments are organized as follows: We firstly showcase the extrapolation of NNs-Hp in learning some common functions in Section 4.1. Next, we assess the extrapolation performance on non-synthetic dataset in Section 4.2 and conduct the experiment in learning spherical harmonics in Section 4.3. Due to the constrained space, the extrapolation in a visual analogy task and the spectral bias in image classification task are deferred to Appendix E.5 and Appendix E.6, respectively.

4.1 Extrapolation in learning analytically-known functions

These experiments aim to examine the extrapolation behavior of NNs-Hp in regression tasks. Our first experiment includes training the networks via the squared loss to fit several well-known and analytically-known underlying functions. During prediction, we sample data points beyond the training regime and observe the extrapolation performance. More details on implementation can be found in Appendix E.1. We set the target function as $f_{\rho}(x) = x^3 + x^2 - 10x + 5$ and use four-layer fully-connected NN. As presented in Figure 1(a) and Figure 1(b), fully-connected NN extrapolates linearly while NN-Hp approximates better the extrapolation part of the underlying non-linear function, which are consistent with Theorem 4 and Theorem 5.

Learning $f_{\rho}(x) = \cos(2x)$. We choose eleven-layer fully-connected NN. The training set and testing set are the same as in the previous experiment. Observing Figure 1(c) and Figure 1(d), we find that NN-Hp is more flexible to learn the non-linear function outside the training region while fully-connected NN still extrapolates linearly.

Learning $f_{\rho}(\mathbf{x}) = (x^{(1)})^2 + (x^{(2)})^2$, where $x^{(1)}$ and $x^{(2)}$ is the first and second dimension of $\mathbf{x} \in \mathbb{R}^2$. In this task, we choose three-layer NNs. Each model is trained with different data distribution, i.e.,

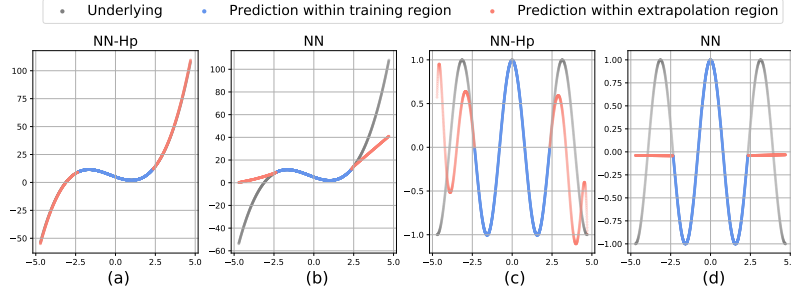


Figure 1: **Extrapolation function.** The blue curve indicates the training regime while the pink color symbolizes the extrapolation regime. (a) and (b) show the fitting results towards $f_\rho(x) = x^3 + x^2 - 10x + 5$. We can see that NN extrapolates linearly without the Hadamard product (Hp) while NN-Hp is able to extrapolate to the underlying non-linear function nearly. (c) and (d) present the fitting results towards $f_\rho(x) = \cos(2x)$. Notably, NN-Hp is more flexible to learn the non-linear function outside the training region.

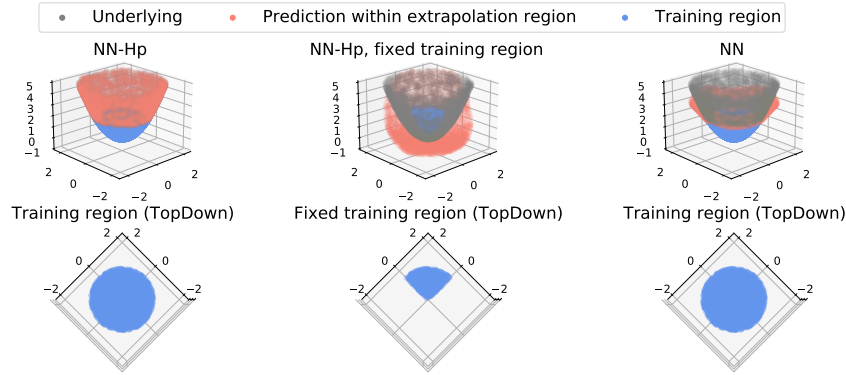


Figure 2: Fitting results for the underlying function $f_\rho(x) = (x^{(1)})^2 + (x^{(2)})^2$, where $x^{(1)}$ and $x^{(2)}$ are the first and second dimension of $x \in R^2$. Blue points indicate the training regime, pink points symbolize the extrapolation regime, gray points indicate the underlying function. **Left:** We train NNs-Hp with the training set containing support in all directions, the network is able to extrapolate successfully. **Middle:** We train NN-Hp with the training set wherein two dimensions of the data are fixed to be positive, NN-Hp fails to extrapolate. **Right:** We remove the Hadamard product of the network, which leads to linear extrapolation.

the training set contains support in all directions in the first case while two dimension of the training set are fixed to be positive in the second case. The result is visually depicted in Figure 2, which shows that NNs-Hp can achieve exact extrapolation if the training set contains support in all directions and thereby validates Theorem 6. On the other hand, NNs without the Hadamard product fail to extrapolate to the underlying function due to its linear extrapolation.

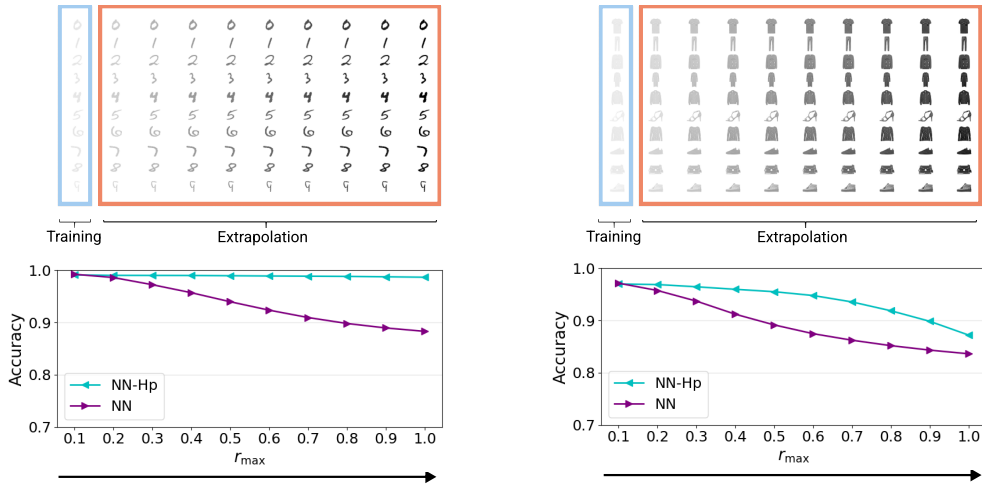
4.2 Extrapolation in real-world dataset

In this section, we assess the extrapolation performance beyond synthetic datasets.

Variation of brightness. This experiment is conducted on two well-known grayscale image datasets: MNIST dataset [LeCun et al., 1998] and Fashion-MNIST dataset Xiao et al. [2017]. For these two datasets, the original range of the pixel of each image is $[0, 1]$, we divided it by 10 for the raw training set to construct the new one where the pixels range from 0 to 0.1. During extrapolation, we limit the range of the original testing set to $[0, r_{\max}]$ through division, where $r_{\max} \in \{0.1, 0.2, 0.3, \dots, 1.0\}$, as illustrated in the top two panels in Figure 3. Then we feed these images into the trained network and evaluate the accuracy. More details on the implementation can be found in Appendix E.2. The accuracy is summarized in the two bottom plots of Figure 3. We find that both networks achieve

similar accuracy in the case $r_{\max} = 0.1$ while inserting Hadamard product (Hp) into NN improves the performance during extrapolation.

Arithmetic extrapolation. Now we turn to a more challenging task. As human we can usually extrapolate to arbitrarily large numbers in arithmetic. How do the neural networks perform during extrapolation? Following the setup of Bloice et al. [2020], we use MNIST dataset, where there are 100 different two-image combinations of the digits $0 \sim 9$. We randomly pick up 90 combinations as the training set and the remaining 10 combinations as the extrapolation set. This problem is treated as regression instead of classification for higher error tolerance following Bloice et al. [2020]. In addition, if we design the network as a classifier, the number of the class will vary as the change of the splitting for the training set and testing set. The network only outputs one single discrete value. However, we still measure the accuracy by rounding the network output. five-layer fully-connected NNs and convolution NNs are chosen as the baselines. For comparison, we implement NN-Hp with dense layers and NN-Hp with convolution layers, respectively. More details on the implementation can be found in the Appendix E.3. The results obtained by a three-fold cross validation are summarized in Table 1, where we can see NN-Hp has a better extrapolation behavior in such more difficult task.



(a) Examples and results on MNIST dataset.

(b) Examples and results on Fashion-MNIST dataset.

Figure 3: The top two panels show the examples of extrapolation in MNIST dataset and Fashion-MNIST dataset. r_{\max} varies from 0.1 to 1.0. from left to right, indicating the variation of the darkness of the image. The bottom two panels show the accuracy as r_{\max} increasing. Both networks achieve similar accuracy in the case $r_{\max} = 0.1$ while inserting Hadamard product (Hp) into NN improves the performance during extrapolation.

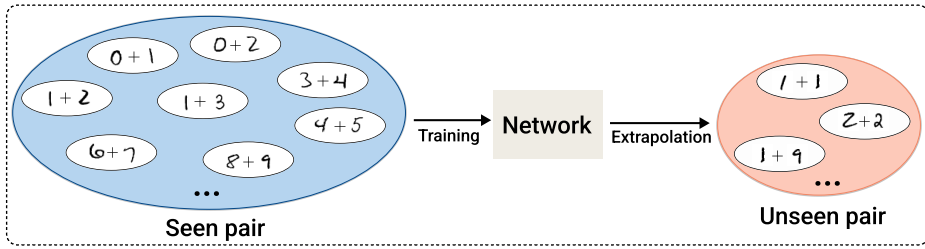


Figure 4: A schematic illustration for the task of arithmetic extrapolation.

4.3 Spectral bias in learning spherical harmonics

Here, we aim to learn the linear combinations of spherical Harmonics where inputs are sampled from the uniform distribution on the unit sphere. Our experiment follows the setup in Choraria et al. [2022], which only considers NNs-Hp with one Hadamard product. The target function is

Table 1: Results in the task of arithmetic extrapolation, which aims to predict the target label with regression. 'Interpolation' indicates the accuracy in the seen pairs during training while 'Extrapolation' indicates the accuracy tested in those unseen pairs. Three ways are used for the network output: (a) Rounding, the output is rounded to the nearest integer. (b) Floor/ceiling, A floor and ceiling function is applied for the output and if one of those equals to the ground truth label, we treat it as a correct prediction. (c) ± 1 . An error of ± 1 is allowed. We can observe that NN-Hp has a better extrapolation behavior compared with the baselines.

Method		Rounding	Floor/ceiling	± 1
NN(Dense)	Interpolation	0.980 ± 0.002	0.999 ± 0.000	0.999 ± 0.000
	Extrapolation	0.436 ± 0.065	0.805 ± 0.042	0.887 ± 0.011
NN-Hp (Dense)	Interpolation	0.926 ± 0.031	0.996 ± 0.001	0.999 ± 0.000
	Extrapolation	0.554 ± 0.011	0.802 ± 0.010	0.889 ± 0.008
NN(Conv)	Interpolation	0.945 ± 0.983	0.983 ± 0.021	0.994 ± 0.007
	Extrapolation	0.617 ± 0.103	0.918 ± 0.016	0.953 ± 0.006
NN-Hp (Conv)	Interpolation	0.991 ± 0.002	0.998 ± 0.000	0.999 ± 0.000
	Extrapolation	0.825 ± 0.109	0.948 ± 0.006	0.963 ± 0.007

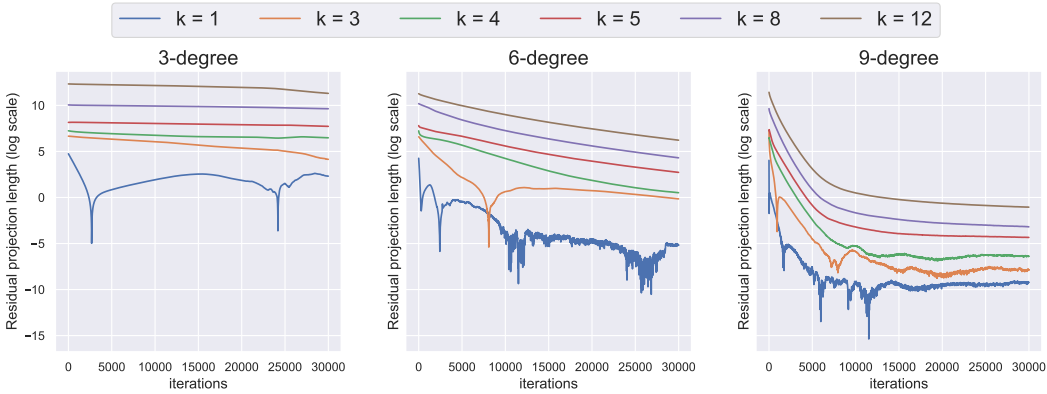


Figure 5: Comparison of convergence curve of error projection lengths for NNs-Hp with N -degree multiplicative interactions, where $N \in \{3, 6, 9\}$ for different order harmonics with $K \in \{1, 3, 4, 5, 8, 12\}$. We can see the improvement for high-degree interactions in the rate of convergence of error.

defined by: $f^*(\mathbf{x}) = \frac{1}{N(\mathcal{K})} \sum_{k \in \mathcal{K}} A_k P_k(\langle \mathbf{x}, \zeta_k \rangle)$, $\mathcal{K} = \{1, 3, 4, 5, 8, 12\}$, where $P_k(t)$ denotes the k -degree Gegenbauer polynomial, ζ_k are fixed vectors that are independently sampled from uniform distribution on unit sphere, and $N(\mathcal{K})$ is the normalizing constant. The error residuals with different \mathcal{K} are compared during the training process. Implementation details are deferred to Appendix E.4. In this experiment, we show that increasing the number of multiplicative interactions can improve the rate of convergence of error, as presented in Figure 5.

5 Conclusion

This paper examines neural network with Hadamard product with a particular focus on polynomial neural networks from a theoretical perspective. The analysis of the NTK paves the way for knowing interesting properties of the networks, such as the extrapolation behavior and the spectral bias. Experimental results in learning analytically-known functions validate our hypothesis. We further conduct several experiments in real-world datasets and demonstrate the advantage of inserting Hadamard products into standard neural networks. We believe not only our framework provides a good justification for a deeper understanding of neural architecture, but it also lays the foundations to investigate other more complicated OOD problems such as domain adaption and invariant learning in future work.

Acknowledgements

We are thankful to the reviewers for providing constructive feedback. This project has received support from the European Research Council (ERC) under the European Union’s Horizon 2020 research and innovation programme (grant agreement number 725594 - timedata). This work was sponsored by the Army Research Office and was accomplished under Grant Number W911NF-19-1-0404. This work was supported by Zeiss. This work has received funding from SNF project – Deep Optimisation of the Swiss National Science Foundation (SNSF) under grant number 200021_205011. This work was supported by Hasler Foundation Program: Hasler Responsible AI (project number 21043).

References

- Sina Alemohammad, Zichao Wang, Randall Balestriero, and Richard Baraniuk. The recurrent neural tangent kernel. In *International Conference on Learning Representations (ICLR)*, 2021.
- Zeyuan Allen-Zhu, Yuanzhi Li, and Zhao Song. A convergence theory for deep learning via over-parameterization. In *International Conference on Machine Learning (ICML)*, pages 242–252. PMLR, 2019.
- Martin Arjovsky, Léon Bottou, Ishaan Gulrajani, and David Lopez-Paz. Invariant risk minimization. *arXiv preprint arXiv:1907.02893*, 2019.
- Sanjeev Arora, Simon S Du, Wei Hu, Zhiyuan Li, Russ R Salakhutdinov, and Ruosong Wang. On exact computation with an infinitely wide neural net. *Advances in neural information processing systems (NeurIPS)*, 32, 2019.
- Francesca Babiloni, Ioannis Marras, Filippos Kokkinos, Jiankang Deng, Grigorios Chrysos, and Stefanos Zafeiriou. Poly-nl: Linear complexity non-local layers with 3rd order polynomials. In *International Conference on Computer Vision (ICCV)*, 2021.
- Francis Bach. Breaking the curse of dimensionality with convex neural networks. *The Journal of Machine Learning Research*, 18(1):629–681, 2017.
- Randall Balestriero, Jerome Pesenti, and Yann LeCun. Learning in high dimension always amounts to extrapolation. *arXiv preprint arXiv:2110.09485*, 2021.
- Etienne Barnard and LFA Wessels. Extrapolation and interpolation in neural network classifiers. *IEEE Control Systems Magazine*, 12(5):50–53, 1992.
- Yuval Belfer, Amnon Geifman, Meirav Galun, and Ronen Basri. Spectral analysis of the neural tangent kernel for deep residual networks. *arXiv preprint arXiv:2104.03093*, 2021.
- Alberto Bietti and Julien Mairal. On the inductive bias of neural tangent kernels. In *Advances in neural information processing systems (NeurIPS)*, 2019.
- Marcus D Bloice, Peter M Roth, and Andreas Holzinger. Performing arithmetic using a neural network trained on digit permutation pairs. In *International Symposium on Methodologies for Intelligent Systems*, pages 255–264. Springer, 2020.
- Antony Browne. Representation and extrapolation in multilayer perceptrons. *Neural computation*, 14(7):1739–1754, 2002.
- W.M. Campbell and C.C. Broun. Using polynomial networks for speech recognition. In *Neural Networks for Signal Processing X. Proceedings of the 2000 IEEE Signal Processing Society Workshop (Cat. No.00TH8501)*, volume 2, pages 795–803 vol.2, 2000. doi: 10.1109/NNSP.2000.890159.
- Yuan Cao, Zhiying Fang, Yue Wu, Ding-Xuan Zhou, and Quanquan Gu. Towards understanding the spectral bias of deep learning. *arXiv preprint arXiv:1912.01198*, 2019.
- L Carlitz. The product of two ultraspherical polynomials. *Glasgow Mathematical Journal*, 5(2): 76–79, 1961.

- Lenaic Chizat, Edouard Oyallon, and Francis Bach. On lazy training in differentiable programming. *Advances in neural information processing systems (NeurIPS)*, 32, 2019.
- Moulik Choraria, Leello Tadesse Dadi, Grigorios Chrysos, Julien Mairal, and Volkan Cevher. The spectral bias of polynomial neural networks. In *International Conference on Learning Representations (ICLR)*, 2022.
- Grigorios Chrysos, Stylianos Moschoglou, Yannis Panagakis, and Stefanos Zafeiriou. Polygan: High-order polynomial generators. *arXiv preprint arXiv:1908.06571*, 2019.
- Grigorios Chrysos, Markos Georgopoulos, and Yannis Panagakis. Conditional generation using polynomial expansions. In *Advances in neural information processing systems (NeurIPS)*, 2021a.
- Grigorios G. Chrysos, Stylianos Moschoglou, Giorgos Bouritsas, Yannis Panagakis, Jiankang Deng, and Stefanos Zafeiriou. P-nets: Deep polynomial neural networks. In *Conference on Computer Vision and Pattern Recognition (CVPR)*, 2020.
- Grigorios G. Chrysos, Stylianos Moschoglou, Giorgos Bouritsas, Jiankang Deng, Yannis Panagakis, and Stefanos P Zafeiriou. Deep polynomial neural networks. *IEEE Transactions on Pattern Analysis and Machine Intelligence (T-PAMI)*, 2021b.
- Grigorios G Chrysos, Markos Georgopoulos, Jiankang Deng, Jean Kossaifi, Yannis Panagakis, and Anima Anandkumar. Augmenting deep classifiers with polynomial neural networks. In *European Conference on Computer Vision (ECCV)*, 2022.
- Amit Daniely, Roy Frostig, and Yoram Singer. Toward deeper understanding of neural networks: The power of initialization and a dual view on expressivity. In *Advances in neural information processing systems (NeurIPS)*, 2016.
- Alexander G. de G. Matthews, Jiri Hron, Mark Rowland, Richard E. Turner, and Zoubin Ghahramani. Gaussian process behaviour in wide deep neural networks. In *International Conference on Learning Representations (ICLR)*, 2018.
- Simon Du, Jason Lee, Haochuan Li, Liwei Wang, and Xiyu Zhai. Gradient descent finds global minima of deep neural networks. In *International Conference on Machine Learning (ICML)*, 2019a.
- Simon S Du, Kangcheng Hou, Russ R Salakhutdinov, Barnabas Poczos, Ruosong Wang, and Keyulu Xu. Graph neural tangent kernel: Fusing graph neural networks with graph kernels. *Advances in neural information processing systems (NeurIPS)*, 32, 2019b.
- Simon S Du, Xiyu Zhai, Barnabas Poczos, and Aarti Singh. Gradient descent provably optimizes over-parameterized neural networks. In *International Conference on Learning Representations (ICLR)*, 2019c.
- Feng-Lei Fan, Mengzhou Li, Fei Wang, Rongjie Lai, and Ge Wang. Expressivity and trainability of quadratic networks. *arXiv preprint arXiv:2110.06081*, 2021.
- Rizal Fathony, Anit Kumar Sahu, Devin Willmott, and J Zico Kolter. Multiplicative filter networks. In *International Conference on Learning Representations (ICLR)*, 2021.
- Christopher Frye and Costas J Efthimiou. Spherical harmonics in p dimensions. *arXiv preprint arXiv:1205.3548*, 2012.
- Pamela J Haley and DONALD Soloway. Extrapolation limitations of multilayer feedforward neural networks. In *International Joint Conference on Neural Networks*, volume 4, pages 25–30. IEEE, 1992.
- Kaixuan Huang, Yuqing Wang, Molei Tao, and Tuo Zhao. Why do deep residual networks generalize better than deep feedforward networks?—a neural tangent kernel perspective. *Advances in neural information processing systems (NeurIPS)*, 33:2698–2709, 2020.
- Alexey Grigorevich Ivakhnenko. Polynomial theory of complex systems. *IEEE transactions on Systems, Man, and Cybernetics*, 1971.

- Arthur Jacot, Franck Gabriel, and Clement Hongler. Neural tangent kernel: Convergence and generalization in neural networks. In S. Bengio, H. Wallach, H. Larochelle, K. Grauman, N. Cesa-Bianchi, and R. Garnett, editors, *Advances in neural information processing systems (NeurIPS)*. Curran Associates, Inc., 2018.
- Siddhant M. Jayakumar, Wojciech M. Czarnecki, Jacob Menick, Jonathan Schwarz, Jack Rae, Simon Osindero, Yee Whye Teh, Tim Harley, and Razvan Pascanu. Multiplicative interactions and where to find them. In *International Conference on Learning Representations (ICLR)*, 2020.
- Tero Karras, Samuli Laine, and Timo Aila. A style-based generator architecture for generative adversarial networks. In *Conference on Computer Vision and Pattern Recognition (CVPR)*, 2019.
- Diederik P. Kingma and Jimmy Ba. Adam: A method for stochastic optimization. In *International Conference on Learning Representations (ICLR)*, 2015.
- Tamara G Kolda and Brett W Bader. Tensor decompositions and applications. *SIAM review*, 2009.
- Wouter M Kouw and Marco Loog. A review of domain adaptation without target labels. *IEEE transactions on pattern analysis and machine intelligence*, 43(3):766–785, 2019.
- Mark A Kramer and JA Leonard. Diagnosis using backpropagation neural networks—analysis and criticism. *Computers & chemical engineering*, 14(12):1323–1338, 1990.
- Yann LeCun, Léon Bottou, Yoshua Bengio, Patrick Haffner, et al. Gradient-based learning applied to document recognition. *Proceedings of the IEEE*, 86(11):2278–2324, 1998.
- Jaehoon Lee, Lechao Xiao, Samuel Schoenholz, Yasaman Bahri, Roman Novak, Jascha Sohl-Dickstein, and Jeffrey Pennington. Wide neural networks of any depth evolve as linear models under gradient descent. In *Advances in neural information processing systems (NeurIPS)*, volume 32, 2019.
- Georg Martius and Christoph H Lampert. Extrapolation and learning equations. *arXiv preprint arXiv:1610.02995*, 2016.
- Quynh Nguyen, Marco Mondelli, and Guido F Montufar. Tight bounds on the smallest eigenvalue of the neural tangent kernel for deep relu networks. In *International Conference on Machine Learning (ICML)*, pages 8119–8129, 2021.
- Nasim Rahaman, Aristide Baratin, Devansh Arpit, Felix Draxler, Min Lin, Fred Hamprecht, Yoshua Bengio, and Aaron Courville. On the spectral bias of neural networks. In *International Conference on Machine Learning (ICML)*, 2019.
- Elan Rosenfeld, Pradeep Kumar Ravikumar, and Andrej Risteski. The risks of invariant risk minimization. In *International Conference on Learning Representations (ICLR)*, 2021.
- Subham Sahoo, Christoph Lampert, and Georg Martius. Learning equations for extrapolation and control. In *International Conference on Machine Learning (ICML)*, pages 4442–4450, 2018.
- David Saxton, Edward Grefenstette, Felix Hill, and Pushmeet Kohli. Analysing mathematical reasoning abilities of neural models. *arXiv preprint arXiv:1904.01557*, 2019.
- Zheyuan Shen, Jiashuo Liu, Yue He, Xingxuan Zhang, Renzhe Xu, Han Yu, and Peng Cui. Towards out-of-distribution generalization: A survey. *arXiv preprint arXiv:2108.13624*, 2021.
- Yoan Shin and Joydeep Ghosh. The pi-sigma network: An efficient higher-order neural network for pattern classification and function approximation. In *International Joint Conference on Neural Networks*, 1991.
- Jiahao Su, Wonmin Byeon, Jean Kossaifi, Furong Huang, Jan Kautz, and Anima Anandkumar. Convolutional tensor-train lstm for spatio-temporal learning. *Advances in neural information processing systems (NeurIPS)*, 33:13714–13726, 2020.
- Tom Tirer, Joan Bruna, and Raja Giryes. Kernel-based smoothness analysis of residual networks. *arXiv preprint arXiv:2009.10008*, 2020.

- Jan H van Schuppen. *Control and System Theory of Discrete-Time Stochastic Systems*. Springer, 2021.
- Roman Vershynin. Introduction to the non-asymptotic analysis of random matrices. *arXiv preprint arXiv:1011.3027*, 2010.
- Xiaolong Wang, Ross Girshick, Abhinav Gupta, and Kaiming He. Non-local neural networks. In *Conference on Computer Vision and Pattern Recognition (CVPR)*, 2018.
- Taylor Webb, Zachary Dulberg, Steven Frankland, Alexander Petrov, Randall O’Reilly, and Jonathan Cohen. Learning representations that support extrapolation. In *International Conference on Machine Learning (ICML)*, pages 10136–10146. PMLR, 2020.
- Blake Woodworth, Suriya Gunasekar, Jason D Lee, Edward Moroshko, Pedro Savarese, Itay Golan, Daniel Soudry, and Nathan Srebro. Kernel and rich regimes in overparametrized models. In *Conference on Learning Theory*, pages 3635–3673. PMLR, 2020.
- Han Xiao, Kashif Rasul, and Roland Vollgraf. Fashion-mnist: a novel image dataset for benchmarking machine learning algorithms. *arXiv preprint arXiv:1708.07747*, 2017.
- Keyulu Xu, Mozhi Zhang, Jingling Li, Simon Shaolei Du, Ken-Ichi Kawarabayashi, and Stefanie Jegelka. How neural networks extrapolate: From feedforward to graph neural networks. In *International Conference on Learning Representations (ICLR)*, 2021.
- Huiming Zhang and Song Xi Chen. Concentration inequalities for statistical inference. *arXiv preprint arXiv:2011.02258*, 2020.
- Zhenyu Zhu, Fabian Latorre, Grigorios Chrysos, and Volkan Cevher. Controlling the complexity and lipschitz constant improves polynomial nets. In *International Conference on Learning Representations (ICLR)*, 2022.
- Difan Zou, Yuan Cao, Dongruo Zhou, and Quanquan Gu. Gradient descent optimizes over-parameterized deep relu networks. *Machine learning*, 2020.

Contents of the Appendix

The Appendix is organized as follows:

- In Appendix A.1, we provide a theoretical overview for a specific family of neural networks with Hadamard product, called Π -Nets. The background in neural tangent kernel (NTK) is elaborated in Appendix A.2.
- The derivations and the proofs for the NTK of PNNs are further elaborated in Appendix B, including the formulation of NTK, the width requirement for the empirical kernel to converge to NTK at initialization, and the equivalent to kernel regression.
- The proof for extrapolation-related theorem is included in Appendix C.
- In Appendix D, we present the proof for the decay rate of eigenvalues of the NTK of PNNs.
- Details on the experiment are developed in Appendix E.
- In Appendix F and G, we extend this analysis beyond the class of polynomial neural networks.
- Societal impact and limitations of this work are discussed in Appendix H and I, respectively.

A Theoretical background

Our analysis in the main paper is built on a specific family of neural network with Hadamard product, called Π -Nets. In Appendix A.1, we will overview the theoretical background of Π -Nets. Next, in Appendix A.2, we briefly introduce the background on neural tangent kernel (NTK), which is used for analyzing the networks. We start with introducing some notation. The *mode- m* vector product of a M^{th} order tensor $\mathcal{A} \in \mathbb{R}^{J_1 \times J_2 \times \dots \times J_{m-1} \times J_m \times J_{m+1} \times \dots \times J_M}$ and a vector $\mathbf{x} \in \mathbb{R}^{J_m}$ is denoted by $\mathcal{A} \times_m \mathbf{x} \in \mathbb{R}^{J_1 \times J_2 \times \dots \times J_{m-1} \times J_{m+1} \times \dots \times J_M}$, resulting in $(M-1)^{\text{th}}$ order tensor:

$$(\mathcal{A} \times_m \mathbf{x})_{j_1, \dots, j_{m-1}, j_{m+1}, \dots, j_M} = \sum_{j_m=1}^{J_m} a_{j_1, j_2, \dots, j_M} z_{j_m}.$$

The *mode- m* vector product of a tensor and multiple vectors is denoted as:

$$\mathcal{A} \times_1 \mathbf{x}^{(1)} \times_2 \mathbf{x}^{(2)} \times_3 \dots \times_M \mathbf{x}^{(M)} = \mathcal{A} \prod_{m=1}^M \times_m \mathbf{x}^{(m)}.$$

In *CANDECOMP/PARAFAC (CP) decomposition* [Kolda and Bader, 2009], the tensor is decomposed into a sum of component rank-one tensors. The rank- R CP decomposition of an M^{th} order tensor \mathcal{A} is symbolized by

$$\mathcal{A} = \sum_{r=1}^R \mathbf{x}_r^{(1)} \circ \mathbf{x}_r^{(2)} \circ \dots \circ \mathbf{x}_r^{(M)}, \quad (6)$$

where \circ is the outer product of vectors.

Table 2: Core symbols

Symbol	Dimension(s)	Definition
$\sigma(\cdot), \dot{\sigma}(\cdot)$	-	ReLU function and its derivative
$\odot, *$	-	Khatri-Rao product, Hadamard product
\mathbf{e}_j	\mathbb{R}^m	j^{th} canonical basis vector of \mathbb{R}^m
n, N	\mathbb{N}	Polynomial term degree and total degree
\mathbf{x}	\mathbb{R}^d	Input to the network
$f(\mathbf{x})$	\mathbb{R}	Output of the network
$\mathcal{A}^{[n]}$	$\mathbb{R}^{1 \times \prod_{i=1}^n \times_i d}$	Parameter tensor of the polynomial
$\mathbf{b}, \mathbf{W}_n, \mathbf{W}_{N+1}$	$\mathbb{R}, \mathbb{R}^{m \times d}, \mathbb{R}^{1 \times m}$	Learnable parameters
$\ell_2(\boldsymbol{\theta}) = \frac{1}{2} \sum_{(\mathbf{x}_i, y_i) \in (\mathcal{X}, \mathcal{Y})} (f(\mathbf{x}_i; \boldsymbol{\theta}) - y_i)^2$	\mathbb{R}	Empirical training loss
$\{\mathbf{x}_i\}_{i=1}^{ \mathcal{X} }, \{y_i\}_{i=1}^{ \mathcal{Y} }$		Features and labels of training set $(\mathcal{X}, \mathcal{Y})$

A.1 A Primer on polynomial nets

The goal of II-Nets is to learn an N -degree polynomial expansion that outputs $f(\mathbf{x}) \in \mathbb{R}^d$ with respect to the input $\mathbf{x} \in \mathbb{R}^d$:

$$f(\mathbf{x}) = \sum_{n=1}^N \left(\mathcal{A}^{[n]} \prod_{j=2}^{n+1} \times_j \mathbf{x} \right) + \mathbf{b}, \quad (7)$$

where $\left\{ \mathcal{A}^{[n]} \in \mathbb{R}^{1 \times \prod_{i=1}^n \times_i d} \right\}_{n=1}^N$ and $\mathbf{b} \in \mathbb{R}$ are learnable parameters. Nevertheless, as the degree of the polynomial increases, the number of parameters in Eq. (7) grows exponentially. In order to improve the scalability, a coupled CP decomposition (CCP) with factor sharing is used to reduce parameters [Kolda and Bader, 2009, Chrysos et al., 2021b]. With CCP, all the weight tensors $\{\mathcal{A}^{[n]}\}_{n=1}^N$ are jointly factorized by a coupled CP decomposition where the factors between different degrees are shared. For instance, the parameters of the third degree expansion follows:

- First degree parameters: $\mathbf{A}^{[1]} = \mathbf{W}_4 \mathbf{W}_1$.
- Second degree parameters: $\mathbf{A}_{(1)}^{[2]} = \mathbf{W}_4 (\mathbf{W}_3 \odot \mathbf{W}_1) + \mathbf{W}_4 (\mathbf{W}_2 \odot \mathbf{W}_1)$.
- Third degree parameters: $\mathbf{A}_{(1)}^{[3]} = \mathbf{W}_4 (\mathbf{W}_3 \odot \mathbf{W}_2 \odot \mathbf{W}_1)$.

Combining the aforementioned factorizations, the third degree expansion of Eq. (7) can be expressed as:

$$f(\mathbf{x}) = \mathbf{b} + \mathbf{W}_4 \mathbf{W}_1 \mathbf{x} + \mathbf{W}_4 (\mathbf{W}_3 \odot \mathbf{W}_1) (\mathbf{x} \odot \mathbf{x}) + \mathbf{W}_4 (\mathbf{W}_2 \odot \mathbf{W}_1) (\mathbf{x} \odot \mathbf{x}) + \mathbf{W}_4 (\mathbf{W}_3 \odot \mathbf{W}_2 \odot \mathbf{W}_1) (\mathbf{x} \odot \mathbf{x} \odot \mathbf{x}). \quad (8)$$

Next, we introduce the following lemma used to convert the Khatri-Rao products into a Hadamard product.

Lemma 2. [Chrysos et al., 2019] Given two sets of real-valued matrices $\{\mathbf{A}_\nu \in \mathbb{R}^{I_\nu \times K}\}_{\nu=1}^N$ and $\{\mathbf{B}_\nu \in \mathbb{R}^{I_\nu \times L}\}_{\nu=1}^N$, the following equality holds:

$$\left(\bigodot_{\nu=1}^N \mathbf{A}_\nu \right)^\top \cdot \left(\bigodot_{\nu=1}^N \mathbf{B}_\nu \right) = (\mathbf{A}_1^\top \cdot \mathbf{B}_1) * \dots * (\mathbf{A}_N^\top \cdot \mathbf{B}_N). \quad (9)$$

Applying the above lemma on Eq. (8), we obtain:

$$f(\mathbf{x}) = \mathbf{b} + \mathbf{W}_4 \{ (\mathbf{W}_3 \mathbf{x}) * [(\mathbf{W}_2 \mathbf{x}) * (\mathbf{W}_1 \mathbf{x}) + \mathbf{W}_1 \mathbf{x}] + (\mathbf{W}_2 \mathbf{x}) * (\mathbf{W}_1 \mathbf{x}) + \mathbf{W}_1 \mathbf{x} \}, \quad (10)$$

which can be further converted to the following recursive relationship and generalized to arbitrary degree:

$$\begin{aligned} \mathbf{y}_n &= (\mathbf{W}_n \mathbf{x}) * \mathbf{y}_{n-1} + \mathbf{y}_{n-1}, \quad n = 2, \dots, N \\ \mathbf{y}_1 &= \mathbf{W}_1 \mathbf{x}, \quad f(\mathbf{x}) = \mathbf{W}_{N+1} \mathbf{y}_N + \mathbf{b}. \end{aligned} \quad (11)$$

The parameters $\mathbf{b} \in \mathbb{R}$, $\mathbf{W}_{N+1} \in \mathbb{R}^{1 \times m}$, $\mathbf{W}_n \in \mathbb{R}^{d \times m}$ for $n = 1, \dots, N$, are learnable. To simplify the proof, we follow Zhu et al. [2022] to reparameterize Eq. (11) and obtain Eq. (1) (in the main body). Apart from CCP, we can also factorize the polynomial networks by other decompositions. The recursive formula of NCP is:

$$\begin{aligned} \mathbf{y}_n &= (\mathbf{W}_n \mathbf{x}) * (\mathbf{F}_n^T \mathbf{y}_{n-1} + \mathbf{B}_n^T \mathbf{b}_n), \quad n = 2, \dots, N \\ \mathbf{y}_1 &= (\mathbf{W}_1 \mathbf{x}) * (\mathbf{B}_1^T \mathbf{b}_1), \quad f(\mathbf{x}) = \mathbf{W}_{N+1} \mathbf{y}_N + \mathbf{b}, \end{aligned} \quad (12)$$

where the parameters \mathbf{b} , \mathbf{W}_{N+1} , \mathbf{W}_n , \mathbf{B}_n , \mathbf{b}_n , \mathbf{F}_n are learnable. The recursive formula of NCP-skip is:

$$\begin{aligned} \mathbf{y}_n &= (\mathbf{W}_n \mathbf{x}) * (\mathbf{F}_n^T \mathbf{y}_{n-1} + \mathbf{B}_n^T \mathbf{b}_n) + \mathbf{D}_n \mathbf{y}_{n-1}, \quad n = 2, \dots, N \\ \mathbf{y}_1 &= (\mathbf{W}_1 \mathbf{x}) * (\mathbf{B}_1^T \mathbf{b}_1), \quad f(\mathbf{x}) = \mathbf{W}_{N+1} \mathbf{y}_N + \mathbf{b}, \end{aligned} \quad (13)$$

where the parameters \mathbf{b} , \mathbf{W}_{N+1} , \mathbf{W}_n , \mathbf{B}_n , \mathbf{b}_n , \mathbf{F}_n , \mathbf{D}_n are learnable.

A.2 A Primer on NTK

In this section, we summarize how training a neural network by minimizing squared loss, i.e., $\ell_2(\boldsymbol{\theta}_t) = \frac{1}{2} \sum_{(\mathbf{x}_i, y_i) \in (\mathcal{X}, \mathcal{Y})} (f(\mathbf{x}_i; \boldsymbol{\theta}_t) - y_i)^2$, via gradient descent can be characterized by the kernel regression predictor with NTK.

By choosing an infinitesimally small learning rate, we can obtain the following gradient flow:

$$\frac{d\boldsymbol{\theta}_t}{dt} = -\nabla \ell_2(\boldsymbol{\theta}_t).$$

By substituting the loss into the above equation and using the chain rule, we can find that the network outputs $f(\boldsymbol{\theta}_t) = \text{vec}(\{f(\mathbf{x}_i; \boldsymbol{\theta}_t)\}_{\mathbf{x}_i \in \mathcal{X}}) \in \mathbb{R}^{|\mathcal{X}|}$ admit the following dynamics:

$$\frac{df(\boldsymbol{\theta}_t)}{dt} = -\hat{\mathbf{K}}_t(f(\boldsymbol{\theta}_t) - \mathbf{y}), \quad (14)$$

where $\mathbf{y} = \text{vec}(\{y_i\}_{y_i \in \mathcal{Y}}) \in \mathbb{R}^{|\mathcal{X}|}$, $\hat{\mathbf{K}}_t = J(\boldsymbol{\theta}_t)J(\boldsymbol{\theta}_t)^\top = \left(\frac{\partial f(\boldsymbol{\theta}_t)}{\partial \boldsymbol{\theta}}\right) \left(\frac{\partial f(\boldsymbol{\theta}_t)}{\partial \boldsymbol{\theta}}\right)^\top \in \mathbb{R}^{|\mathcal{X}| \times |\mathcal{X}|}$. Jacot et al. [2018], Arora et al. [2019] have shown that for fully-connected neural networks, under the infinite-width setting and proper initialization, $\hat{\mathbf{K}}_t$ will keep constant during training and $\hat{\mathbf{K}}_0$ will converge to a fixed matrix $\mathbf{K} \in \mathbb{R}^{|\mathcal{X}| \times |\mathcal{X}|}$, where $K_{ij} = K(\mathbf{x}_i, \mathbf{x}_j)$ is the NTK value for the inputs \mathbf{x}_i and \mathbf{x}_j . Then, based on $\hat{\mathbf{K}}_t = \hat{\mathbf{K}}_0 = \mathbf{K}$, we can rewrite Eq. (14) as:

$$\frac{df(\boldsymbol{\theta}_t)}{dt} = -\mathbf{K}(f(\boldsymbol{\theta}_t) - \mathbf{y}). \quad (15)$$

This implies the network output for any $\mathbf{x} \in \mathbb{R}^d$ can be calculated by the kernel regression predictor with the associated NTK:

$$f(\mathbf{x}) = (K(\mathbf{x}, \mathbf{x}_1), \dots, K(\mathbf{x}, \mathbf{x}_{|\mathcal{X}|})) \cdot \mathbf{K}^{-1} \mathbf{y},$$

where $K(\mathbf{x}, \mathbf{x}_i)$ is the kernel value between test data \mathbf{x} and training data \mathbf{x}_i .

B Proofs of NTK

We derive the NTK of NNs-Hp with multiple multiplicative interactions in Appendix B.1. Next, we prove the width requirement for the empirical kernel to converge to NTK at initialization in Appendix B.2. Lastly, we analyze the training dynamics of NNs-Hp under gradient descent in Appendix B.3.

B.1 Proof of Theorem 1

Recall that the NTK is defined as the limit of the following inner product:

$$\mathbf{K}(\mathbf{x}, \mathbf{x}') = \lim_{m \rightarrow \infty} \langle \nabla_{\boldsymbol{\theta}} f_{\boldsymbol{\theta}}(\mathbf{x}), \nabla_{\boldsymbol{\theta}} f_{\boldsymbol{\theta}}(\mathbf{x}') \rangle,$$

where $\boldsymbol{\theta}$ represents all the parameters. Observing Eq. (1), we can compute the gradient with respect to each weight and then sum up the inner products to obtain the NTK.

Below, we denote by $\tilde{\boldsymbol{\alpha}}_n = \mathbf{W}_n \mathbf{x}$, $n \in [N]$ the pre-activation vectors and $\boldsymbol{\alpha}_n$ the vectors after applying the element-wise ReLU activation to $\tilde{\boldsymbol{\alpha}}_n$.

Firstly, we compute the contribution to the NTK w.r.t \mathbf{W}_1 , its corresponding derivative is as follows:

$$\begin{aligned} \partial_{\mathbf{W}_1} f(\mathbf{x}) &= \sqrt{\frac{2}{m}} \sum_{j=1}^m W_{N+1}^{(j)} \left(\prod_{n=2}^N \sigma \left(\sqrt{\frac{2}{m}} \tilde{\boldsymbol{\alpha}}_n^{(j)}(\mathbf{x}) \right) \right) \dot{\sigma} \left(\sqrt{\frac{2}{m}} \tilde{\boldsymbol{\alpha}}_1^{(j)}(\mathbf{x}) \right) \partial_{\mathbf{W}_1} \tilde{\boldsymbol{\alpha}}_1^{(j)}(\mathbf{x}) \\ &= \sqrt{\frac{2}{m}} \sum_{j=1}^m W_{N+1}^{(j)} \left(\prod_{n=2}^N \sigma \left(\sqrt{\frac{2}{m}} \tilde{\boldsymbol{\alpha}}_n^{(j)}(\mathbf{x}) \right) \right) \dot{\sigma} \left(\sqrt{\frac{2}{m}} \tilde{\boldsymbol{\alpha}}_1^{(j)}(\mathbf{x}) \right) \partial_{\mathbf{W}_1} (\mathbf{e}_j^\top \mathbf{W}_N \mathbf{x}) \\ &= \sqrt{\frac{2}{m}} \sum_{j=1}^m W_{N+1}^{(j)} \left(\prod_{n=2}^N \sigma \left(\sqrt{\frac{2}{m}} \tilde{\boldsymbol{\alpha}}_n^{(j)}(\mathbf{x}) \right) \right) \dot{\sigma} \left(\sqrt{\frac{2}{m}} \tilde{\boldsymbol{\alpha}}_1^{(j)}(\mathbf{x}) \right) (\mathbf{e}_j \mathbf{x}^\top). \end{aligned}$$

The inner product of the derivative is:

$$\begin{aligned}
& \langle \partial_{\mathbf{W}_1} f(\mathbf{x}), \partial_{\mathbf{W}_1} f(\mathbf{x}') \rangle \\
&= \frac{2}{m} \sum_{j,k=1}^m W_{N+1}^{(j)} W_{N+1}^{(k)} \left(\prod_{n=2}^N \left(\frac{2}{m} \sigma(\tilde{\alpha}_n^{(j)}(\mathbf{x})) \sigma(\tilde{\alpha}_n^{(j)}(\mathbf{x}')) \right) \right) \left(\frac{2}{m} \dot{\sigma}(\tilde{\alpha}_1^{(j)}(\mathbf{x})) \dot{\sigma}(\tilde{\alpha}_1^{(k)}(\mathbf{x}')) \right) \langle \mathbf{e}_j \mathbf{x}^\top, \mathbf{e}_k \mathbf{x}'^\top \rangle \\
&= \frac{2}{m} \sum_{j,k=1}^m W_{N+1}^{(j)} W_{N+1}^{(k)} \left(\prod_{n=2}^N \left(\frac{2}{m} \sigma(\tilde{\alpha}_n^{(j)}(\mathbf{x})) \sigma(\tilde{\alpha}_n^{(k)}(\mathbf{x}')) \right) \right) \left(\frac{2}{m} \dot{\sigma}(\tilde{\alpha}_1^{(j)}(\mathbf{x})) \dot{\sigma}(\tilde{\alpha}_1^{(k)}(\mathbf{x}')) \right) \mathbf{x}^\top \mathbf{x}' \delta_{jk} \\
&= \frac{2}{m} \sum_{j=1}^m W_{N+1}^{(j)} W_{N+1}^{(j)} \left(\prod_{n=2}^N \left(\frac{2}{m} \sigma(\tilde{\alpha}_n^{(j)}(\mathbf{x})) \sigma(\tilde{\alpha}_n^{(j)}(\mathbf{x}')) \right) \right) \left(\frac{2}{m} \dot{\sigma}(\tilde{\alpha}_1^{(j)}(\mathbf{x})) \dot{\sigma}(\tilde{\alpha}_1^{(j)}(\mathbf{x}')) \right) \mathbf{x}^\top \mathbf{x}'.
\end{aligned} \tag{16}$$

By the law of large numbers and the fact that $\mathbb{E}_{w \sim \mathcal{N}(0,1)} w^2 = 1$, we obtain:

$$\lim_{m \rightarrow \infty} \langle \partial_{\mathbf{W}_1} f(\mathbf{x}), \partial_{\mathbf{W}_1} f(\mathbf{x}') \rangle = 2 \langle \mathbf{x}, \mathbf{x}' \rangle \kappa_1(\mathbf{x}, \mathbf{x}') (\kappa_2(\mathbf{x}, \mathbf{x}'))^{N-1}, \tag{17}$$

where κ_1 and κ_2 are defined in Eq. (3). Given that Eq. (1) is symmetric w.r.t $\{\mathbf{W}_n\}_{n=1}^N$, the contributions of $\{\mathbf{W}_n\}_{n=1}^N$ to the NTK are the same, we can trivially multiply Eq. (17) by N .

Next, we compute the contribution to the NTK w.r.t \mathbf{W}_{N+1} , its corresponding derivative is as follows:

$$\partial_{\mathbf{W}_{N+1}} f(\mathbf{x}) = \sqrt{\frac{2}{m}} \left(\sqrt{\frac{2}{m}} \sigma(\tilde{\alpha}_N) * \dots * \sqrt{\frac{2}{m}} \sigma(\tilde{\alpha}_1) \right).$$

The inner product of the derivative is:

$$\langle \partial_{\mathbf{W}_{N+1}} f(\mathbf{x}), \partial_{\mathbf{W}_{N+1}} f(\mathbf{x}') \rangle = \frac{2}{m} \sum_{j=1}^m \left(\prod_{n=1}^N \left(\frac{2}{m} \sigma(\tilde{\alpha}_n^{(j)}(\mathbf{x})) \sigma(\tilde{\alpha}_n^{(j)}(\mathbf{x}')) \right) \right).$$

By the law of large numbers:

$$\begin{aligned}
& \lim_{m \rightarrow \infty} \langle \partial_{\mathbf{W}_{N+1}} f(\mathbf{x}), \partial_{\mathbf{W}_{N+1}} f(\mathbf{x}') \rangle \\
&= 2 \left(\mathbb{E}_{\mathbf{w} \sim \mathcal{N}(\mathbf{0}, \frac{2}{m} \mathbf{I})} (\sigma(\mathbf{w}^\top \mathbf{x}) \cdot \sigma(\mathbf{w}^\top \mathbf{x}')) \right)^N \\
&= 2 \cdot (\kappa_2(\mathbf{x}, \mathbf{x}'))^N.
\end{aligned} \tag{18}$$

The proof is completed by multiplying Eq. (17) by N and adding by Eq. (18).

B.2 Proof of Theorem 2

Before we prove Theorem 2, we need to tackle a technical key issue: how to provide probability estimates for the multiplication of several sub-exponential random variables. To this end, we introduce sub-Weibull random variables in the following definition, which allows for our case and still admits exponential decay tails.

Definition 2 (Sub-Weibull distributions Zhang and Chen [2020]). Given positive constants a, b , a random variable X is sub-Weibull if it satisfies $P(|X| \geq x) \leq ae^{-bx^\theta}$, where $\theta > 0$ is the order.

Remark: The classical sub-exponential and sub-Gaussian random variables are sub-Weibull by taking $\theta = 1$ and $\theta = 2$, respectively.

Based on the definition above, we have the following concentration inequality on sub-Weibull random variables.

Lemma 3 (Sub-Weibull Concentration Zhang and Chen [2020]). Given some $\theta > 0$, if $\{X_k\}_{k=1}^K$ are independent mean zero random variable such that the sub-Weibull norm $\|X_k\|_{\psi_\theta} < \infty$ for all $1 \leq k \leq K$, then for any weight vector $\mathbf{w} = (w_1, \dots, w_K) \in \mathbb{R}^n$, for any $\zeta \in (0, 1)$ one has

$$P\left(\left| \sum_{k=1}^K w_k X_k \right| \geq 2\epsilon\rho(\theta) \|\mathbf{b}\|_2 \{ \sqrt{\zeta} + D(\theta)\zeta^{1/\theta} \} \right) \leq 2e^{-\zeta},$$

where $\mathbf{b} = (w_1 \|X_1\|_{\psi_\theta}, \dots, w_K \|X_K\|_{\psi_\theta})^\top$, $D(\theta) := \frac{4^{1/\theta}}{\sqrt{2}\|\mathbf{b}\|_2} \times \begin{cases} \|\mathbf{b}\|_\infty, & \text{if } \theta < 1, \\ 4e\|\mathbf{b}\|_{\frac{\theta}{1-\theta}}/C(\theta), & \text{if } \theta \geq 1, \end{cases}$

$$\rho(\theta) := \max\{\sqrt{2}, 2^{1/\theta}\} \times \begin{cases} \sqrt{8}e^3(2\pi)^{1/4}e^{1/24}(e^{2/e}/\theta)^{1/\theta}, & \text{if } \theta < 1, \\ 4e + 2(\log 2)^{1/\theta}, & \text{if } \theta \geq 1. \end{cases}$$

Proof of Theorem 2. Recall from Eq. (16):

$$\begin{aligned} & \langle \partial_{\mathbf{W}_1} f(\mathbf{x}), \partial_{\mathbf{W}_1} f(\mathbf{x}') \rangle \\ &= \frac{1}{m} \sum_{k=1}^m \underbrace{2W_{N+1}^{(k)} W_{N+1}^{(k)} \left(\prod_{n=2}^N \left(\frac{2}{m} \sigma(\tilde{\alpha}_n^{(k)}(\mathbf{x})) \sigma(\tilde{\alpha}_n^{(k)}(\mathbf{x}')) \right) \right)}_{:= X_k} \left(\frac{2}{m} \dot{\sigma}(\tilde{\alpha}_1^{(k)}(\mathbf{x})) \dot{\sigma}(\tilde{\alpha}_1^{(k)}(\mathbf{x}')) \right) \mathbf{x}^\top \mathbf{x}', \end{aligned}$$

where $\tilde{\alpha}_n = \mathbf{W}_n \mathbf{x}$, $n = 1, \dots, N$ represent the pre-activation. Firstly, we centralize X_k and denote by \widehat{X}_k as follows:

$$\widehat{X}_k = X_k - 2\kappa_1(\mathbf{x}, \mathbf{x}')(\kappa_2(\mathbf{x}, \mathbf{x}'))^{N-1} \mathbf{x}^\top \mathbf{x}'$$

Since all the weight matrices \mathbf{W}_n , $n = 1, \dots, N+1$ are Gaussian, $\sigma(\tilde{\alpha}_n^{(k)}(\mathbf{x}))$, $\sigma(\tilde{\alpha}_n^{(k)}(\mathbf{x}'))$, and $\dot{\sigma}(\tilde{\alpha}_1^{(k)}(\mathbf{x})) \dot{\sigma}(\tilde{\alpha}_1^{(k)}(\mathbf{x}'))$ are sub-Gaussian random variables over the randomness of \mathbf{W}_n ,

Thus, $\{\widehat{X}_k\}_{k=1}^m$ is zero mean sub-Weibull random variable with order $\theta = 2/(2N+1)$. Plugging $w_1, \dots, w_k = 1/m$ into Lemma 3, we get

$$\begin{aligned} \rho\left(\frac{2}{2N+1}\right) &= \sqrt{2}^{2N-1} \sqrt{8}e^3(2\pi)^{1/4}e^{1/24} \left(e^{2/e}(2N-1)/2\right)^{(2N-1)/2} \\ \|\mathbf{b}\|_2 &= \frac{1}{m} \|(\|\widehat{X}_1\|_{\psi_\theta}, \dots, \|\widehat{X}_m\|_{\psi_\theta})\|_2, \quad D\left(\frac{2}{2N+1}\right) = \frac{4^{(2N+1)/2} \|\mathbf{b}\|_\infty}{\sqrt{2} \|\mathbf{b}\|_2}. \end{aligned}$$

Suppose that the width satisfies $m \geq 2^{4N-2} \log^{2N-1}(2N/\delta)$, then for any $\delta \in (0, 1)$, with probability at least $1 - (\delta/N)$ over the randomness of initialization, we have

$$|\langle \partial_{\mathbf{W}_1} f(\mathbf{x}), \partial_{\mathbf{W}_1} f(\mathbf{x}') \rangle - 2\langle \mathbf{x}, \mathbf{x}' \rangle \kappa_1(\mathbf{x}, \mathbf{x}') (\kappa_2(\mathbf{x}, \mathbf{x}'))^{N-1}| \leq 4N\rho\left(\frac{2}{2N+1}\right) e\sqrt{\frac{\log(2N/\delta)}{m}}.$$

Note that we only consider one weight matrix above, by applying the union bound, with probability at least $1 - \delta$ over the randomness of initialization, we have:

$$|\langle \nabla f(\mathbf{x}), \nabla f(\mathbf{x}') \rangle - K(\mathbf{x}, \mathbf{x}')| \leq 4N\rho\left(\frac{2}{2N+1}\right) e\sqrt{\frac{\log(2N/\delta)}{m}}.$$

□

B.3 Proof of Theorem 3

Before starting the proof, we introduce the following lemmas that are used to analyze the random initialization of the weight matrices $\mathbf{W}_n \in \mathbb{R}^{m \times d}$, $\forall n \in [N]$ and $\mathbf{W}_{N+1} \in \mathbb{R}^{1 \times m}$.

Lemma 4. [Vershynin, 2010, Corollary 5.35] For a weight matrix $\mathbf{W} \in \mathbb{R}^{m \times d}$ where each element is sampled independently from $\mathcal{N}(0, 1)$, for every $\zeta \geq 0$, with probability at least $1 - 2\exp(-\zeta^2/2)$ one has:

$$\sqrt{m} - \sqrt{d} - \zeta \leq \lambda_{\min}(\mathbf{W}) \leq \lambda_{\max}(\mathbf{W}) \leq \sqrt{m} + \sqrt{d} + \zeta,$$

where $\lambda_{\max}(\mathbf{W})$ and $\lambda_{\min}(\mathbf{W})$ represents the largest and smallest singular value of \mathbf{W} , respectively.

Next, we will show the local boundness and the local Lipschitzness of the Jacobian. We use $\|\cdot\|_F$ and $\|\cdot\|$ to represent the Frobenius norm and spectral norm of a matrix, respectively. The Euclidean norm of a vector is symbolized by $\|\cdot\|_2$.

Lemma 5. Consider the N -degree NNs-Hp in Eq. (1), assume the input $\mathbf{x} \in \mathbb{R}^d$ is bounded $\|\mathbf{x}\|_2 \leq 1$, then there exists $\gamma_1 > 0$, $\gamma_2 > 0$ (both are independent of the width m) such that for every $r > 0$, $\delta \in (0, 1)$, $m \geq \left(r + \sqrt{d} + 2 \log((2N + 2)/\delta)\right)^2$, with probability at least $1 - \delta$ over the random initialization, the following holds for all $\boldsymbol{\theta}, \tilde{\boldsymbol{\theta}} \in D(\boldsymbol{\theta}, r) := \{\boldsymbol{\theta} : \|\boldsymbol{\theta} - \boldsymbol{\theta}_0\|_2 \leq r\}$

$$\|J(\boldsymbol{\theta})\|_F \leq \gamma_1, \quad (19)$$

$$\|J(\boldsymbol{\theta}) - J(\tilde{\boldsymbol{\theta}})\|_F \leq \gamma_2 \|\boldsymbol{\theta} - \tilde{\boldsymbol{\theta}}\|_2. \quad (20)$$

Proof of Lemma 5. Based on Lemma 4 and union bound, when $m \geq \left(r + \sqrt{d} + 2 \log((2N + 2)/\delta)\right)^2$, with probability at least $1 - \delta$ for any $\delta \in (0, 1)$, the following inequalities hold for all $n = 1, \dots, N$ simultaneously:

$$\|\mathbf{W}_n\| \leq \sqrt{m} + \sqrt{d} + \delta \leq 2\sqrt{m},$$

$$\|\mathbf{W}_{N+1}\| \leq \sqrt{m} + 1 + \delta \leq 2\sqrt{m},$$

$$\begin{aligned} \|\widehat{\mathbf{W}}_n\| &= \|\mathbf{W}_n + \Delta\mathbf{W}_n\| \leq \|\mathbf{W}_n\| + \|\Delta\mathbf{W}_n\| \leq \sqrt{m} + \sqrt{d} + \delta + \|\Delta\mathbf{W}_n\|_F \\ &\leq \sqrt{m} + \sqrt{d} + \delta + \|\Delta\boldsymbol{\theta}\|_2 \leq \sqrt{m} + \sqrt{d} + \delta + r \leq 2\sqrt{m}. \end{aligned}$$

Below, we abbreviate the description of probability and the width requirement since the following events rely on the same random initialization of the weight matrices. The following shorthand notations are made:

$$\begin{aligned} \widetilde{\mathbf{T}}_n &= \left(\sqrt{\frac{2}{m}} \sigma(\widetilde{\mathbf{W}}_n \mathbf{x}) * \dots * \sqrt{\frac{2}{m}} \sigma(\widetilde{\mathbf{W}}_1 \mathbf{x}) \right), \\ \mathbf{T}_n &= \left(\sqrt{\frac{2}{m}} \sigma(\mathbf{W}_n \mathbf{x}) * \dots * \sqrt{\frac{2}{m}} \sigma(\mathbf{W}_1 \mathbf{x}) \right). \end{aligned}$$

Firstly, we prove the local boundness (Eq. (19)). Given that Eq. (1) is symmetric w.r.t $\{\mathbf{W}_i\}_{i=1}^N$, we start with calculating the bound with respect of one of the parameter matrix \mathbf{W}_N . The derivate is:

$$\begin{aligned} \partial_{\mathbf{W}_N} f(\mathbf{x}) &= \left(\frac{2}{\sqrt{m}} \mathbf{W}_{N+1} * \frac{2}{\sqrt{m}} \dot{\sigma}(\mathbf{W}_N \mathbf{x}) * \frac{2}{\sqrt{m}} \sigma(\mathbf{W}_{N-1} \mathbf{x}) * \dots * \frac{2}{\sqrt{m}} \sigma(\mathbf{W}_1 \mathbf{x}) \right) \mathbf{x}^\top \\ &= \left(\frac{2}{\sqrt{m}} \mathbf{W}_{N+1} * \frac{2}{\sqrt{m}} \dot{\sigma}(\mathbf{W}_N \mathbf{x}) * \mathbf{T}_{N-1} \right) \mathbf{x}^\top. \end{aligned}$$

Its Frobenius norm satisfies with probability:

$$\begin{aligned} \|\partial_{\mathbf{W}_N} f(\mathbf{x})\|_F &= \left\| \left(\frac{2}{\sqrt{m}} \mathbf{W}_{N+1} * \frac{2}{\sqrt{m}} \dot{\sigma}(\mathbf{W}_N \mathbf{x}) * \mathbf{T}_{N-1} \right) \mathbf{x}^\top \right\|_F \\ &\leq \left\| \frac{2}{\sqrt{m}} \mathbf{W}_{N+1} * \frac{2}{\sqrt{m}} \dot{\sigma}(\mathbf{W}_N \mathbf{x}) * \mathbf{T}_{N-1} \right\|_2 \\ &\leq \left\| \frac{2}{\sqrt{m}} \mathbf{W}_{N+1} \right\|_2 \left\| \frac{2}{\sqrt{m}} \dot{\sigma}(\mathbf{W}_N \mathbf{x}) \right\|_2 \|\mathbf{T}_{N-1}\|_2 \\ &\leq 4 \left\| \frac{2}{\sqrt{m}} \dot{\sigma}(\mathbf{W}_N \mathbf{x}) \right\|_2 \|\mathbf{T}_{N-1}\|_2 \\ &\leq 8 \|\mathbf{T}_{N-1}\|_2 \leq 2^{2N+1}, \end{aligned}$$

where the second and the third inequality use the Cauchy-Schwarz inequality, the last inequality is based on the upper bound of $\|\mathbf{T}_{N-1}\|_2$, which holds with probability:

$$\|\mathbf{T}_{N-1}\|_2 = \left\| \frac{2}{\sqrt{m}} \sigma(\mathbf{W}_{N-1} \mathbf{x}) * \dots * \frac{2}{\sqrt{m}} \sigma(\mathbf{W}_1 \mathbf{x}) \right\|_2 \leq \left\| \frac{2}{\sqrt{m}} \sigma(\widehat{\mathbf{W}} \mathbf{x}) \right\|_2^{N-1} \quad (21)$$

$$\leq \left(\frac{2}{\sqrt{m}} \|\widehat{\mathbf{W}}\| \right)^{N-1} \leq \left| \frac{2}{\sqrt{m}} 2\sqrt{m} \right|^{N-1} = 4^{N-1}, \quad (22)$$

where $\widehat{\mathbf{W}} \in \mathbb{R}^{m \times d}$ is sampled from $\mathcal{N}(\mathbf{0}, \mathbf{1})$. Now we consider all the weight matrices except \mathbf{W}_{N+1} that is not trained. We have the following bound with probability:

$$\|J(\boldsymbol{\theta})\|_F = \sqrt{\sum_{\mathbf{x} \in \mathcal{X}} \left(\sum_{n=1}^N \left\| \frac{\partial f(\mathbf{x}; \boldsymbol{\theta})}{\partial \mathbf{W}_n} \right\|_F^2 \right)} \leq 2^{2N+1} \sqrt{N|\mathcal{X}|} = \gamma_1,$$

where γ_1 does not depend on the width m . This completes the first part of the proof.

Next, we prove the local Lipschitzness (Eq. (19)). Similarly, since Eq. (1) is symmetric w.r.t $\{\mathbf{W}_i\}_{i=1}^N$, firstly, we calculate the perturbation with respect of one of the parameter matrix \mathbf{W}_N . The following inequality holds with probability:

$$\begin{aligned} & \left\| \partial_{\widetilde{\mathbf{W}}_N} f(\mathbf{x}) - \partial_{\mathbf{W}_N} f(\mathbf{x}) \right\|_F & (23) \\ & = \left\| \left(\frac{2}{\sqrt{m}} \mathbf{W}_{N+1} * \frac{2}{\sqrt{m}} \dot{\sigma}(\widetilde{\mathbf{W}}_N \mathbf{x}) * \widetilde{\mathbf{T}}_{N-1} \right) \mathbf{x}^\top - \left(\frac{2}{\sqrt{m}} \mathbf{W}_{N+1} * \frac{2}{\sqrt{m}} \dot{\sigma}(\mathbf{W}_N \mathbf{x}) * \mathbf{T}_{N-1} \right) \mathbf{x}^\top \right\|_F & (24) \end{aligned}$$

$$\leq \left\| \frac{2}{\sqrt{m}} \mathbf{W}_{N+1} * \frac{2}{\sqrt{m}} \dot{\sigma}(\widetilde{\mathbf{W}}_N \mathbf{x}) * \widetilde{\mathbf{T}}_{N-1} - \frac{2}{\sqrt{m}} \mathbf{W}_{N+1} * \frac{2}{\sqrt{m}} \dot{\sigma}(\mathbf{W}_N \mathbf{x}) * \mathbf{T}_{N-1} \right\|_2 \|\mathbf{x}\|_2 \quad (25)$$

$$\leq \left\| \frac{2}{\sqrt{m}} \mathbf{W}_{N+1} \right\|_2 \left\| \frac{2}{\sqrt{m}} \dot{\sigma}(\widetilde{\mathbf{W}}_N \mathbf{x}) * \widetilde{\mathbf{T}}_{N-1} - \frac{2}{\sqrt{m}} \dot{\sigma}(\mathbf{W}_N \mathbf{x}) * \mathbf{T}_{N-1} \right\|_2 \quad (26)$$

$$\leq 4 \left\| \frac{2}{\sqrt{m}} \dot{\sigma}(\widetilde{\mathbf{W}}_N \mathbf{x}) * \widetilde{\mathbf{T}}_{N-1} - \frac{2}{\sqrt{m}} \dot{\sigma}(\mathbf{W}_N \mathbf{x}) * \mathbf{T}_{N-1} \right\|_2 \quad (27)$$

$$\leq 4 \left\| \left(\frac{2}{\sqrt{m}} \dot{\sigma}(\mathbf{W}_N \mathbf{x}) - \frac{2}{\sqrt{m}} \dot{\sigma}(\widetilde{\mathbf{W}}_N \mathbf{x}) \right) * \mathbf{T}_{N-1} \right\|_2 + 4 \left\| \frac{2}{\sqrt{m}} \dot{\sigma}(\widetilde{\mathbf{W}}_N \mathbf{x}) * (\mathbf{T}_{N-1} - \widetilde{\mathbf{T}}_{N-1}) \right\|_2 \quad (28)$$

$$\leq 4 \left\| \left(\frac{2}{\sqrt{m}} \dot{\sigma}(\widetilde{\mathbf{W}}_N \mathbf{x}) - \frac{2}{\sqrt{m}} \dot{\sigma}(\mathbf{W}_N \mathbf{x}) \right) \right\|_2 \|\mathbf{T}_{N-1}\|_2 + 4 \left\| \frac{2}{\sqrt{m}} \dot{\sigma}(\widetilde{\mathbf{W}}_N \mathbf{x}) \right\|_2 \|\mathbf{T}_{N-1} - \widetilde{\mathbf{T}}_{N-1}\|_2 \quad (29)$$

$$\leq \frac{8}{\sqrt{m}} \|\widetilde{\mathbf{W}}_N \mathbf{x} - \mathbf{W}_N \mathbf{x}\|_2 \|\mathbf{T}_{N-1}\|_2 + 8 \|\mathbf{T}_{N-1} - \widetilde{\mathbf{T}}_{N-1}\|_2 \quad (30)$$

$$\leq \frac{8}{\sqrt{m}} \|\widetilde{\mathbf{W}}_N - \mathbf{W}_N\| \|\mathbf{T}_{N-1}\|_2 + 8 \|\mathbf{T}_{N-1} - \widetilde{\mathbf{T}}_{N-1}\|_2, \quad (31)$$

where Eq. (25) is due to $\|\mathbf{a}\mathbf{b}^\top\|_F \leq \|\mathbf{a}\|_2 \|\mathbf{b}\|_2$ for two arbitrary vectors \mathbf{a} and \mathbf{b} , Eq. (28) comes from triangle inequality, Eq. (30) is based on Lipschitz continuous gradient of the ReLU activation function. Using the result in Eq. (22) and the following inequality:

$$\|\widetilde{\mathbf{W}}_N - \mathbf{W}_N\| \leq \|\widetilde{\mathbf{W}}_N - \mathbf{W}_N\|_F \leq \|\boldsymbol{\theta} - \widetilde{\boldsymbol{\theta}}\|_2.$$

The first term in Eq. (31) can be bounded with probability by:

$$\frac{8}{\sqrt{m}} \|\widetilde{\mathbf{W}}_N - \mathbf{W}_N\| \|\mathbf{T}_{N-1}\|_2 \leq \frac{2^{2N+1}}{\sqrt{m}} \|\boldsymbol{\theta} - \widetilde{\boldsymbol{\theta}}\|_2.$$

For the second term in Eq. (31), we will bound $\|\widetilde{\mathbf{T}}_{N-1} - \mathbf{T}_{N-1}\|_2$ by induction. Base case satisfies with probability:

$$\begin{aligned} \|\widetilde{\mathbf{T}}_1 - \mathbf{T}_1\|_2 &= \left\| \frac{2}{\sqrt{m}} \sigma(\widetilde{\mathbf{W}}_1 \mathbf{x}) - \frac{2}{\sqrt{m}} \sigma(\mathbf{W}_1 \mathbf{x}) \right\|_2 \leq \left\| \frac{2}{\sqrt{m}} (\widetilde{\mathbf{W}}_1 \mathbf{x} - \mathbf{W}_1 \mathbf{x}) \right\|_2 \\ &\leq \frac{2}{\sqrt{m}} \|\widetilde{\mathbf{W}}_1 - \mathbf{W}_1\| \leq \frac{2}{\sqrt{m}} \|\boldsymbol{\theta} - \widetilde{\boldsymbol{\theta}}\|_2, \end{aligned}$$

Assume $\|\tilde{\mathbf{T}}_n - \mathbf{T}_n\|_2 \leq \frac{C_2}{\sqrt{m}} \|\boldsymbol{\theta} - \tilde{\boldsymbol{\theta}}\|_2$, then, with probability:

$$\begin{aligned}
& \|\tilde{\mathbf{T}}_{n+1} - \mathbf{T}_{n+1}\|_2 \\
& \leq \left\| \frac{2}{\sqrt{m}} \sigma(\tilde{\mathbf{W}}_{n+1} \mathbf{x}) * (\tilde{\mathbf{T}}_n - \mathbf{T}_n) \right\|_2 + \left\| \mathbf{T}_n * \frac{2}{\sqrt{m}} (\sigma(\tilde{\mathbf{W}}_{n+1} \mathbf{x}) - \sigma(\mathbf{W}_{n+1} \mathbf{x})) \right\|_2 \\
& \leq \frac{2}{\sqrt{m}} \|\sigma(\tilde{\mathbf{W}}_{n+1} \mathbf{x})\|_2 \frac{C_2}{\sqrt{m}} \|\tilde{\boldsymbol{\theta}} - \boldsymbol{\theta}\|_2 + \frac{2}{\sqrt{m}} \|\mathbf{T}_n\|_2 \|\sigma(\tilde{\mathbf{W}}_{n+1} \mathbf{x}) - \sigma(\mathbf{W}_{n+1} \mathbf{x})\|_2 \\
& \leq \frac{2}{\sqrt{m}} \|\tilde{\mathbf{W}}_{n+1}\| \frac{C_2}{\sqrt{m}} \|\tilde{\boldsymbol{\theta}} - \boldsymbol{\theta}\|_2 + \frac{2^{2n+1}}{\sqrt{m}} \|\Delta \mathbf{W}\| \\
& \leq \frac{2}{\sqrt{m}} \|\tilde{\mathbf{W}}_{n+1}\| \frac{C_2}{\sqrt{m}} \|\tilde{\boldsymbol{\theta}} - \boldsymbol{\theta}\|_2 + \frac{2^{2n+1}}{\sqrt{m}} \|\tilde{\boldsymbol{\theta}} - \boldsymbol{\theta}\|_2 \\
& \leq \frac{2}{\sqrt{m}} 2\sqrt{m} \frac{C_2}{\sqrt{m}} \|\tilde{\boldsymbol{\theta}} - \boldsymbol{\theta}\|_2 + \frac{2^{2n+1}}{\sqrt{m}} \|\tilde{\boldsymbol{\theta}} - \boldsymbol{\theta}\|_2 \\
& \leq \left(\frac{4C_2}{\sqrt{m}} + \frac{2^{2n+1}}{\sqrt{m}} \right) \|\tilde{\boldsymbol{\theta}} - \boldsymbol{\theta}\|_2,
\end{aligned}$$

where the first inequality uses the triangle inequality. Thus, we can bound with probability:

$$\|\tilde{\mathbf{T}}_{N-1} - \mathbf{T}_{N-1}\|_2 \leq \frac{2^{3N-5}}{\sqrt{m}} \|\boldsymbol{\theta} - \tilde{\boldsymbol{\theta}}\|_2.$$

Then Eq. (31) becomes:

$$\|\partial_{\tilde{\mathbf{W}}_N} f(\mathbf{x}) - \partial_{\mathbf{W}_N} f(\mathbf{x})\|_F \leq \frac{8 + 2^{3N-5}}{\sqrt{m}} \|\boldsymbol{\theta} - \tilde{\boldsymbol{\theta}}\|_2.$$

Now we consider all the weight matrices except \mathbf{W}_{N+1} that is not trained. The following inequality holds with probability:

$$\begin{aligned}
\|J(\boldsymbol{\theta}) - J(\tilde{\boldsymbol{\theta}})\|_F &= \sqrt{\sum_{\mathbf{x} \in \mathcal{X}} \left(\sum_{n=1}^N \left\| \frac{\partial f(\mathbf{x}; \boldsymbol{\theta})}{\partial \mathbf{W}_n} - \frac{\partial f(\mathbf{x}; \tilde{\boldsymbol{\theta}})}{\partial \tilde{\mathbf{W}}_n} \right\|_F^2 \right)} \\
&\leq \frac{8 + 2^{3N-5}}{\sqrt{m}} \sqrt{N|\mathcal{X}|} \leq \frac{8 + 2^{3N-5}}{r + \sqrt{d} + 2 \log(2N/\delta)} \sqrt{N|\mathcal{X}|} = \gamma_2,
\end{aligned}$$

where γ_2 does not depend on the width m . This completes the proof of Lemma 5. \square

Finally, note that Theorem 3 is an extension of Lee et al. [2019, Theorem G.1] from MLP to NNs-Hp, the proof of Lemma 5 is quite different for different networks while the idea of the remaining steps is based on the induction rule over time step t , which do not rely on the network. Applying Lemma 5 with $\gamma_1 = \gamma_2 = \frac{3QR_0}{\lambda_{\min}(\mathbf{K})}$ completes the proof, which is similar to the extension from MLPs to ResNets in Tirer et al. [2020, Theorem 5], RNN in Alemohammad et al. [2021, Theorem 2].

C Proofs of extrapolation

C.1 Proof of Theorem 4

Proof of Theorem 4. Recall that an infinite-width neural network trained through gradient descent is equivalent to kernel regression, the network output for any $\mathbf{x} \in \mathbb{R}^d$ is given by

$$f(\mathbf{x}) = (K(\mathbf{x}, \mathbf{x}_1), \dots, K(\mathbf{x}, \mathbf{x}_{|\mathcal{X}|})) \cdot \mathbf{K}^{-1} \mathbf{y},$$

where $\mathbf{K} \in \mathbb{R}^{|\mathcal{X}| \times |\mathcal{X}|}$ is the NTK Gram matrix for training data, $K(\mathbf{x}, \mathbf{x}_i)$ is the kernel value between test data \mathbf{x} and training data \mathbf{x}_i , and $\mathbf{y} \in \mathbb{R}^{|\mathcal{X}|}$ are the training labels. Since the NTK $K(\mathbf{x}, \mathbf{x}')$ is

1-homogeneous w.r.t \mathbf{x} , the network output $f(\mathbf{x})$ is also N -homogeneous w.r.t \mathbf{x} . Therefore, given inputs $\mathbf{x}_0 = t\mathbf{v}$ and $\mathbf{x} = \mathbf{x}_0 + h\mathbf{v}$, the outputs of the network are:

$$\begin{aligned} f(\mathbf{x}_0) &= f(t\mathbf{v}) = t^N \cdot f(\mathbf{v}) \\ f(\mathbf{x}) &= f(((t+h)^N)\mathbf{v}) = (t+h)^N \cdot f(\mathbf{v}), \end{aligned}$$

Thus:

$$f(\mathbf{x}) - f(\mathbf{x}_0) = f(t\mathbf{v}) - f((t+h)\mathbf{v}) = ((t+h)^N - t^N) \cdot f(\mathbf{v}),$$

Thus, the network extrapolates to at most N -degree function with respect to h . \square

C.2 Proof of Theorem 5

Proof of Theorem 5. The NTK of MLPs defined in Section 2.2, denoted by $K^{(N)}(\mathbf{x}, \mathbf{x}')$, can be rewritten in a more compact form [Nguyen et al., 2021]:

$$K^{(N)}(\mathbf{x}, \mathbf{x}') = G^{(N)}(\mathbf{x}, \mathbf{x}') + \sum_{n=1}^{N-1} G^{(n)}(\mathbf{x}, \mathbf{x}') * \dot{G}^{(n+1)}(\mathbf{x}, \mathbf{x}') * \dots * \dot{G}^{(N)}(\mathbf{x}, \mathbf{x}'), \quad (32)$$

where for $n \in [3, N]$:

$$\begin{aligned} K^{(1)}(\mathbf{x}, \mathbf{x}') &= G^{(1)}(\mathbf{x}, \mathbf{x}') = \mathbf{x}^\top \mathbf{x}' \\ G^{(2)}(\mathbf{x}, \mathbf{x}') &= 2\mathbb{E}_{\mathbf{w} \sim \mathcal{N}(0, \mathbf{I})} [\sigma(\mathbf{w}^\top \mathbf{x}) \sigma(\mathbf{w}^\top \mathbf{x}')] \\ G^{(n)}(\mathbf{x}, \mathbf{x}') &= 2\mathbb{E}_{\mathbf{w} \sim \mathcal{N}(0, 1)} \left[\sigma \left(\sqrt{G^{(n-1)}(\mathbf{x}, \mathbf{x}') \mathbf{w}} \right) \sigma \left(\sqrt{G^{(n-1)}(\mathbf{x}, \mathbf{x}') \mathbf{w}} \right) \right], \end{aligned} \quad (33)$$

for $n \in [2, N]$:

$$\begin{aligned} K^{(n)}(\mathbf{x}, \mathbf{x}') &= K^{(n-1)}(\mathbf{x}, \mathbf{x}') * \dot{G}^{(n)}(\mathbf{x}, \mathbf{x}') + G^{(n)}(\mathbf{x}, \mathbf{x}') \\ \dot{G}^{(n)}(\mathbf{x}, \mathbf{x}') &= 2\mathbb{E}_{\mathbf{w} \sim \mathcal{N}(0, 1)} \left[\sigma' \left(\sqrt{G^{(n-1)}(\mathbf{x}, \mathbf{x}') \mathbf{w}} \right) \sigma' \left(\sqrt{G^{(n-1)}(\mathbf{x}, \mathbf{x}') \mathbf{w}} \right) \right]. \end{aligned} \quad (34)$$

Since the ReLU activation function σ is 1-homogeneous and its derivative σ' is 0-homogeneous, $G^{(n)}(\mathbf{x}, \mathbf{x}')$ is 1-homogeneous and $\dot{G}^{(n)}(\mathbf{x}, \mathbf{x}')$ 0-homogeneous w.r.t \mathbf{x} , for $n \in [1, N]$. Thus, the NTK $K^{(N)}(\mathbf{x}, \mathbf{x}')$ is 1-homogeneous w.r.t \mathbf{x} . Since the NTK $K^{(N)}(\mathbf{x}, \mathbf{x}')$ is 1-homogeneous w.r.t \mathbf{x} , the network output $f(\mathbf{x})$ is also 1-homogeneous w.r.t \mathbf{x} . Therefore, given inputs $\mathbf{x}_0 = t\mathbf{v}$ and $\mathbf{x} = \mathbf{x}_0 + h\mathbf{v}$, the outputs of the network are:

$$\begin{aligned} f(\mathbf{x}_0) &= f(t\mathbf{v}) = t \cdot f(\mathbf{v}) \\ f(\mathbf{x}) &= f((t+h)\mathbf{v}) = (t+h) \cdot f(\mathbf{v}) \end{aligned}$$

Thus:

$$f(\mathbf{x}) - f(\mathbf{x}_0) = h \cdot f(\mathbf{v}) \quad (35)$$

Since the term $f(\mathbf{v})$ in Eq. (35) is finite in our assumption, the network extrapolates to a linear function with respect to h . This completes the proof. \square

C.3 Proof of Theorem 6

Lemma 6. A specific feature map $\phi(\mathbf{x})$ induced by the NTK of a two-degree NNs-Hp with ReLU activation function is

$$\begin{aligned} \phi(\mathbf{x}) &= \left(c' \mathbf{x} \cdot \dot{\sigma}(\mathbf{w}^{(k)}, \mathbf{x}) \cdot \sigma(\langle \mathbf{w}^{(k)}, \mathbf{x} \rangle), c'' \sigma(\langle \mathbf{w}^{(k)}, \mathbf{x} \rangle) \cdot \sigma(\langle \mathbf{w}^{(k)}, \mathbf{x} \rangle) \right) \\ &= \left(c' \mathbf{x} \cdot \langle \mathbf{w}^{(k)}, \mathbf{x} \rangle \cdot \dot{\sigma}(\langle \mathbf{w}^{(k)}, \mathbf{x} \rangle), c'' (\langle \mathbf{w}^{(k)}, \mathbf{x} \rangle)^2 \cdot \dot{\sigma}(\langle \mathbf{w}^{(k)}, \mathbf{x} \rangle) \right), \end{aligned} \quad (36)$$

where $\mathbf{w}^{(k)}$ is sampled from $\mathcal{N}(\mathbf{0}, \mathbf{I})$, c' and c'' are constants, the last equality is due to the property of ReLU function: $\sigma(a) = a\dot{\sigma}(a)$ for any $a \in \mathbb{R}$.

Proof of Lemma 6. The NTK for the second degree NNs-Hp with ReLU activation is given by

$$\begin{aligned} \mathbf{K}(\mathbf{x}, \mathbf{x}') &= \frac{8}{m} \cdot \mathbb{E}_{\mathbf{w} \sim \mathcal{N}(\mathbf{0}, \mathbf{I})} (\mathbf{x}^\top \mathbf{x}' \cdot \dot{\sigma}(\mathbf{w}^\top \mathbf{x}) \cdot \dot{\sigma}(\mathbf{w}^\top \mathbf{x}')) \cdot \mathbb{E}_{\mathbf{w} \sim \mathcal{N}(\mathbf{0}, \mathbf{I})} (\sigma(\mathbf{w}^\top \mathbf{x}) \cdot \sigma(\mathbf{w}^\top \mathbf{x}')) \\ &+ \frac{4}{m} \cdot \mathbb{E}_{\mathbf{w} \sim \mathcal{N}(\mathbf{0}, \mathbf{I})} (\sigma(\mathbf{w}^\top \mathbf{x}) \cdot \sigma(\mathbf{w}^\top \mathbf{x}')) \cdot \mathbb{E}_{\mathbf{w} \sim \mathcal{N}(\mathbf{0}, \mathbf{I})} (\sigma(\mathbf{w}^\top \mathbf{x}) \cdot \sigma(\mathbf{w}^\top \mathbf{x}')) . \end{aligned} \quad (37)$$

Then, we utilize the kernel formula to construct the feature map that need to satisfy the following condition:

$$K(\mathbf{x}, \mathbf{x}') = \langle \phi(\mathbf{x}), \phi(\mathbf{x}') \rangle . \quad (38)$$

The following feature map would satisfy Eq. (38) because the inner product of $\phi(\mathbf{x})$ and $\phi(\mathbf{x}')$ for any \mathbf{x}, \mathbf{x}' is equivalent to the expected value in Eq. (37), after integrating with respect to the density function of \mathbf{w} .

$$\begin{aligned} \phi(\mathbf{x}) &= \left(c' \mathbf{x} \cdot \dot{\sigma}(\langle \mathbf{w}^{(k)}, \mathbf{x} \rangle) \cdot \sigma(\langle \mathbf{w}^{(k)}, \mathbf{x} \rangle), c'' \sigma(\langle \mathbf{w}^{(k)}, \mathbf{x} \rangle) \cdot \sigma(\langle \mathbf{w}^{(k)}, \mathbf{x} \rangle) \right) \\ &= \left(c' \mathbf{x} \cdot \langle \mathbf{w}^{(k)}, \mathbf{x} \rangle \cdot \dot{\sigma}(\langle \mathbf{w}^{(k)}, \mathbf{x} \rangle), c'' (\langle \mathbf{w}^{(k)}, \mathbf{x} \rangle)^2 \cdot \dot{\sigma}(\langle \mathbf{w}^{(k)}, \mathbf{x} \rangle) \right) , \end{aligned} \quad (39)$$

where $\mathbf{w}^{(k)}$ is sampled from $\mathcal{N}(\mathbf{0}, \mathbf{I})$, c' and c'' are constants, the last equality is due to the following property of ReLU function: $\sigma(a) = a\dot{\sigma}(a)$ for any $a \in \mathbb{R}$. \square

Sequentially, we are ready to prove Theorem 6.

Proof of Theorem 6. According to Xu et al. [2021, Lemma 2], the kernel regression solution is equivalent to the following form:

$$f(\mathbf{x}) = \boldsymbol{\beta}^\top \phi(\mathbf{x}), \quad (40)$$

where the representation coefficient $\boldsymbol{\beta}$ holds:

$$\begin{aligned} &\min_{\boldsymbol{\beta}'} \|\boldsymbol{\beta}'\|_2 \\ \text{s.t. } &\phi(\mathbf{x}_i)^\top \boldsymbol{\beta}' = y_i, \quad i = 1, \dots, |\mathcal{X}|. \end{aligned} \quad (41)$$

The feature map $\phi(\mathbf{x})$ for a two-degree NNs-Hp with ReLU activation is given in Lemma 6

$$\phi(\mathbf{x}) = \left(c' \mathbf{x} \cdot \langle \mathbf{w}^{(k)}, \mathbf{x} \rangle \cdot \dot{\sigma}(\langle \mathbf{w}^{(k)}, \mathbf{x} \rangle), c'' (\langle \mathbf{w}^{(k)}, \mathbf{x} \rangle)^2 \cdot \dot{\sigma}(\langle \mathbf{w}^{(k)}, \mathbf{x} \rangle) \right) ,$$

where $\mathbf{w}^{(k)}$ is sampled from $\mathcal{N}(\mathbf{0}, \mathbf{I})$, and c', c'' are constant. Below, for avoiding complicating the notation, we will discard the index and use \mathbf{w} to represent a specific $\mathbf{w}^{(k)}$. We assume the constants c' and c'' are 1. Note that $\boldsymbol{\beta}$ consists of weights for each $\mathbf{x} \mathbf{x}^\top \mathbf{w} \cdot \mathbb{I}(\mathbf{w}^\top \mathbf{x} \geq 0) \in \mathbb{R}^d$ and $\mathbf{x} \mathbf{x}^\top \mathbf{w} \mathbf{w}^\top \mathbf{x} \cdot \mathbb{I}(\mathbf{w}^\top \mathbf{x} \geq 0) \in \mathbb{R}$. For any $\mathbf{w} \in \mathbb{R}^d$, the weight vectors corresponding to $\mathbf{x} \mathbf{x}^\top \mathbf{w} \cdot \mathbb{I}(\mathbf{w}^\top \mathbf{x} \geq 0)$ are symbolized by $\hat{\boldsymbol{\beta}}_{\mathbf{w}} = (\hat{\boldsymbol{\beta}}_{\mathbf{w}}^{(1)}, \dots, \hat{\boldsymbol{\beta}}_{\mathbf{w}}^{(k)}) \in \mathbb{R}^d$ and the weight vectors for $\mathbf{x} \mathbf{x}^\top \mathbf{w} \mathbf{w}^\top \mathbf{x} \cdot \mathbb{I}(\mathbf{w}^\top \mathbf{x} \geq 0)$ are symbolized by $\hat{\boldsymbol{\beta}}'_{\mathbf{w}} \in \mathbb{R}$. Given the fact that if $\mathbf{w}^\top \mathbf{x}_i \geq 0$ for any $\mathbf{w} \in \mathbb{R}^d$, then $c\mathbf{w}^\top \mathbf{x}_i \geq 0$ for any $c > 0$, we use the notation $\boldsymbol{\beta}_{\mathbf{w}}$ and $\boldsymbol{\beta}'_{\mathbf{w}}$ to represent the combined effect of all weights $(\hat{\boldsymbol{\beta}}_{c\mathbf{w}}^{(1)}, \dots, \hat{\boldsymbol{\beta}}_{c\mathbf{w}}^{(k)}) \in \mathbb{R}^d$ and $\hat{\boldsymbol{\beta}}'_{c\mathbf{w}} \in \mathbb{R}$ for all $c\mathbf{w}$ with $c > 0$. This allows us to change the distribution of \mathbf{w} from $\mathcal{N}(\mathbf{0}, \mathbf{I}_d)$ to $\text{Unif}(\mathbb{S}^d)$. Specifically, for each $\mathbf{w} \sim \text{Unif}(\mathbb{S}^d)$, $\boldsymbol{\beta}_{\mathbf{w}}^{(j)}$ is denoted as the total effect of the weights in the same direction of \mathbf{w} .

$$\boldsymbol{\beta}_{\mathbf{w}}^{(j)} = \int \hat{\boldsymbol{\beta}}_{\mathbf{u}}^{(j)} \mathbb{I} \left(\frac{\mathbf{w}^\top \mathbf{u}}{\|\mathbf{w}\| \cdot \|\mathbf{u}\|} = 1 \right) d\mathbb{P}(\mathbf{u}), \quad j \in [d]$$

where $\mathbf{u} \sim \mathcal{N}(\mathbf{0}, \mathbf{I})$. Similarly, $\boldsymbol{\beta}'_{\mathbf{w}}$ is defined as follows:

$$\boldsymbol{\beta}'_{\mathbf{w}} = \int \hat{\boldsymbol{\beta}}_{\mathbf{u}} \mathbb{I} \left(\frac{\mathbf{w}^\top \mathbf{u}}{\|\mathbf{w}\| \cdot \|\mathbf{u}\|} = 1 \right) \cdot \|\mathbf{u}\| d\mathbb{P}(\mathbf{u}) \quad (42)$$

Then, the min-norm solution in Eq. (41) is equivalent to:

$$\min_{\beta} \int \left(\beta_w^{(1)} \right)^2 + \left(\beta_w^{(2)} \right)^2 + \dots + \left(\beta_w^{(k)} \right)^2 + (\beta'_w)^2 d\mathbb{P}(\mathbf{w}) \quad (43)$$

$$\text{s.t.} \quad \int_{\mathbf{w}^\top \mathbf{x}_i \geq 0} \mathbf{x}_i^\top \beta_w \mathbf{w}^\top \mathbf{x}_i + \mathbf{x}_i^\top \beta'_w \mathbf{w} \mathbf{w}^\top \mathbf{x}_i d\mathbb{P}(\mathbf{w}) = \mathbf{x}_i^\top \beta_g \mathbf{x}_i \quad \forall i \in [|\mathcal{X}|], \quad (44)$$

where $\mathbf{w} \in \text{Unif}(\mathbb{S}^d)$. Thus, $\mathbb{P}(\mathbf{w})$ is a constant, which indicates that only half of the \mathbf{w} on the unit sphere activate each specific \mathbf{x}_i . Therefore, we can further simplify the constraint in Eq. (44) as

$$\int_{\mathbf{w}^\top \mathbf{x}_i \geq 0} \mathbf{x}_i^\top (\beta_w \mathbf{w}^\top + \beta'_w \mathbf{w} \mathbf{w}^\top - 2\beta_g) \mathbf{x}_i d\mathbb{P}(\mathbf{w}) = 0 \quad \forall i \in [|\mathcal{X}|], \quad (45)$$

where Eq. (45) follows from the following steps

$$\begin{aligned} & \int_{\mathbf{w}^\top \mathbf{x}_i \geq 0} \mathbf{x}_i^\top \beta_w \mathbf{w}^\top \mathbf{x}_i + \mathbf{x}_i^\top \beta'_w \mathbf{w} \mathbf{w}^\top \mathbf{x}_i d\mathbb{P}(\mathbf{w}) = \mathbf{x}_i^\top \beta_g \mathbf{x}_i \quad \forall i \in [|\mathcal{X}|], \\ \Leftrightarrow & \int_{\mathbf{w}^\top \mathbf{x}_i \geq 0} \mathbf{x}_i^\top \beta_w \mathbf{w}^\top \mathbf{x}_i + \mathbf{x}_i^\top \beta'_w \mathbf{w} \mathbf{w}^\top \mathbf{x}_i d\mathbb{P}(\mathbf{w}) \\ & = \frac{1}{\int_{\mathbf{w}^\top \mathbf{x}_i \geq 0} d\mathbb{P}(\mathbf{w})} \cdot \int_{\mathbf{w}^\top \mathbf{x}_i \geq 0} d\mathbb{P}(\mathbf{w}) \cdot \mathbf{x}_i^\top \beta_g \mathbf{x}_i \quad \forall i \in [|\mathcal{X}|], \\ \Leftrightarrow & \int_{\mathbf{w}^\top \mathbf{x}_i \geq 0} \mathbf{x}_i^\top \beta_w \mathbf{w}^\top \mathbf{x}_i + \mathbf{x}_i^\top \beta'_w \mathbf{w} \mathbf{w}^\top \mathbf{x}_i d\mathbb{P}(\mathbf{w}) \\ & = 2 \cdot \int_{\mathbf{w}^\top \mathbf{x}_i \geq 0} \mathbf{x}_i^\top \beta_g \mathbf{x}_i d\mathbb{P}(\mathbf{w}) \quad \forall i \in [|\mathcal{X}|], \\ \Leftrightarrow & \int_{\mathbf{w}^\top \mathbf{x}_i \geq 0} \mathbf{x}_i^\top (\beta_w \mathbf{w}^\top + \beta'_w \mathbf{w} \mathbf{w}^\top - 2\beta_g) \mathbf{x}_i d\mathbb{P}(\mathbf{w}) = 0 \quad \forall i \in [|\mathcal{X}|]. \end{aligned}$$

Lemma 7. *The global optimum of Eq. (43) subject to Eq. (45), i.e.,*

$$\min_{\beta} \int \left(\beta_w^{(1)} \right)^2 + \left(\beta_w^{(2)} \right)^2 + \dots + \left(\beta_w^{(k)} \right)^2 + (\beta'_w)^2 d\mathbb{P}(\mathbf{w}) \quad (46)$$

$$\text{s.t.} \quad \int_{\mathbf{w}^\top \mathbf{x}_i \geq 0} \mathbf{x}_i^\top (\beta_w \mathbf{w}^\top + \beta'_w \mathbf{w} \mathbf{w}^\top - 2\beta_g) \mathbf{x}_i d\mathbb{P}(\mathbf{w}) = 0 \quad \forall i \in [|\mathcal{X}|], \quad (47)$$

satisfies $\beta_w \mathbf{w}^\top + \beta'_w \mathbf{w} \mathbf{w}^\top = 2\beta_g$ for all \mathbf{w} .

Proof of Lemma 7. Through Lemma 7, we can achieve the goal of our proof towards Theorem 6, i.e., $f(\mathbf{x}) = f_\rho(\mathbf{x})$. The reason is that if Lemma 7 holds, for any $\mathbf{x} \in \mathbb{R}^d$:

$$\begin{aligned} f(\mathbf{x}) &= \int_{\mathbf{w}^\top \mathbf{x} \geq 0} \mathbf{x}^\top (\beta_w \mathbf{w}^\top + \beta'_w \mathbf{w} \mathbf{w}^\top) \mathbf{x} d\mathbb{P}(\mathbf{w}) \\ &= \int_{\mathbf{w}^\top \mathbf{x} \geq 0} 2\mathbf{x}^\top \beta_g \mathbf{x} d\mathbb{P}(\mathbf{w}) \\ &= \int_{\mathbf{w}^\top \mathbf{x} \geq 0} d\mathbb{P}(\mathbf{w}) 2\mathbf{x}^\top \beta_g \mathbf{x} \\ &= \frac{1}{2} 2\mathbf{x}^\top \beta_g \mathbf{x} = f_\rho(\mathbf{x}). \end{aligned}$$

Therefore, the remaining step is to prove Lemma 7. Since Eq. (46) is a convex optimization problem with affine constraint Eq. (47), we can introduce the Lagrange multipliers and use the Karush–Kuhn–Tucker (KKT) condition. The Lagrange multiplier has the following form:

$$\mathcal{L}(\beta, \lambda) = \int \left(\beta_w^{(1)} \right)^2 + \left(\beta_w^{(2)} \right)^2 + \dots + \left(\beta_w^{(k)} \right)^2 + (\beta'_w)^2 d\mathbb{P}(\mathbf{w}) \quad (48)$$

$$+ \sum_{i=1}^{|\mathcal{X}|} \lambda_i \cdot \left(\int_{\mathbf{w}^\top \mathbf{x}_i \geq 0} \mathbf{x}_i^\top (\beta_w \mathbf{w}^\top + \beta'_w \mathbf{w} \mathbf{w}^\top - 2\beta_g) \mathbf{x}_i d\mathbb{P}(\mathbf{w}) = 0 \right). \quad (49)$$

By setting the partial derivative to zero, we obtain:

$$\frac{\partial \mathcal{L}}{\partial \beta_{\mathbf{w}}^{(k)}} = 2\beta_{\mathbf{w}}^{(k)} \mathbb{P}(\mathbf{w}) + \sum_{i=1}^{|\mathcal{X}|} \lambda_i \cdot (\mathbf{x}_i \mathbf{x}_i^\top \mathbf{w})^d \cdot \mathbb{I}(\mathbf{w}^\top \mathbf{x}_i \geq 0) = 0 \quad (50)$$

$$\frac{\partial \mathcal{L}}{\partial \beta'_{\mathbf{w}}} = 2\beta'_{\mathbf{w}} \mathbb{P}(\mathbf{w}) + \sum_{i=1}^{|\mathcal{X}|} \lambda_i \cdot \mathbf{x}_i \mathbf{w} \mathbf{w}^\top \mathbf{x}_i \cdot \mathbb{I}(\mathbf{w}^\top \mathbf{x}_i \geq 0) = 0 \quad (51)$$

$$\frac{\partial \mathcal{L}}{\partial \lambda_i} = \int_{\mathbf{w}^\top \mathbf{x}_i \geq 0} \mathbf{x}_i^\top (\beta_{\mathbf{w}} \mathbf{w}^\top + \beta'_{\mathbf{w}} \mathbf{w} \mathbf{w}^\top - 2\beta_g) \mathbf{x}_i \, d\mathbb{P}(\mathbf{w}) = 0. \quad (52)$$

It is obvious that the solution in Lemma 7 satisfies Eq. (52). Thus, the remaining step is to show that there exist a set of λ_i where $i \in [|\mathcal{X}|]$ that satisfies Eq. (50) and Eq. (51). We simplify Eq. (50) and Eq. (51) as follows:

$$\beta_{\mathbf{w}}^{(k)} = c \cdot \sum_{i=1}^{|\mathcal{X}|} \lambda_i \cdot (\mathbf{x}_i \mathbf{x}_i^\top \mathbf{w})^d \cdot \mathbb{I}(\mathbf{w}^\top \mathbf{x}_i \geq 0), \quad (53)$$

$$\beta'_{\mathbf{w}} = c \cdot \sum_{i=1}^{|\mathcal{X}|} \lambda_i \cdot \mathbf{x}_i \mathbf{w} \mathbf{w}^\top \mathbf{x}_i \cdot \mathbb{I}(\mathbf{w}^\top \mathbf{x}_i \geq 0), \quad (54)$$

where c is a constant. Combining Eq. (53) and Eq. (54), we can simplify the constraint Eq. (54) as follows:

$$\beta'_{\mathbf{w}} = \beta_{\mathbf{w}} \mathbf{w}^\top. \quad (55)$$

The remaining step is to show that based on the condition on training data, there exists a set of λ_i that satisfy Eq. (53) and Eq. (55). For each \mathbf{w} , there must exist a set of λ_i so that the following equations satisfy:

$$\beta_{\mathbf{w}}^{(k)} = c \cdot \sum_{i=1}^{|\mathcal{X}|} \lambda_i \cdot (\mathbf{x}_i \mathbf{x}_i^\top \mathbf{w})^d \cdot \mathbb{I}(\mathbf{w}^\top \mathbf{x}_i \geq 0) \quad (56)$$

$$\beta'_{\mathbf{w}} = \beta_{\mathbf{w}}^\top \mathbf{w} \quad (57)$$

$$\beta_{\mathbf{w}} \mathbf{w}^\top + \beta'_{\mathbf{w}} \mathbf{w} \mathbf{w}^\top = 2\beta_g, \quad (58)$$

where β_g and \mathbf{w} are fixed. From Eq. (57) and Eq. (58), we can see that $\beta_{\mathbf{w}}$ is determined by β_g and \mathbf{w} , and there exists a solution for this consistent linear system. Next, we are left with the following linear system that contains d linear equations

$$\beta_{\mathbf{w}}^{(k)} = c \cdot \sum_{i=1}^{|\mathcal{X}|} \lambda_i \cdot (\mathbf{x}_i \mathbf{x}_i^\top \mathbf{w})^d \cdot \mathbb{I}(\mathbf{w}^\top \mathbf{x}_i \geq 0), \quad \forall k \in [d].$$

Recall the assumption for the training data, there exist at least d linearly independent \mathbf{x}_i that activates a specific \mathbf{w} . This implies that for any \mathbf{w} there exists at least d free variables. Thus, the solutions for this linear system exist. \square

Thus, the proof of Theorem 6 is finished. \square

D Proof of spectral bias

Let us recall the core notation. Denote by $\{Y_{k,j}\}_{j=1}^{F(d,k)}$ the k -degree spherical harmonics in $d+1$ variables. $G_k^{(\gamma)}$ represents the Gegenbauer polynomials with respect to the weight function $x \mapsto (1-x^2)^{\gamma-\frac{1}{2}}$ and degree k . Finally, denote by $F(d,k) := \frac{2k+d-1}{k} \binom{k+d-2}{d-1}$.

Given the fact that κ_1 and κ_2 are also dot-product Mercer kernels, their corresponding decompositions in terms of Gegenbauer polynomials can be provided based on Eq. (5):

$$\begin{aligned}\langle \mathbf{x}, \mathbf{x}' \rangle \kappa_1(\mathbf{x}, \mathbf{x}') &= \sum_{k=0}^{\infty} \mu_{1,k} F(d, k) G_k^{(\frac{d-1}{2})}(\langle \mathbf{x}, \mathbf{x}' \rangle) \\ \kappa_2(\mathbf{x}, \mathbf{x}') &= \sum_{k=0}^{\infty} \mu_{2,k} F(d, k) G_k^{(\frac{d-1}{2})}(\langle \mathbf{x}, \mathbf{x}' \rangle).\end{aligned}\tag{59}$$

Note that the decay in $\mu_{1,k} = \mu_{2,k}$ is $\Omega(k^{-d-1})$ [Bach, 2017, Cao et al., 2019, Bietti and Mairal, 2019]. Sequentially, we are ready to prove Theorem 7.

Proof of Theorem 7. For N -degree NNs-Hp, in order to study the decay rate of the eigenvalues, we express the NTK obtained in Eq. (2) as the product of multiple kernels:

$$\begin{aligned}K(\mathbf{x}, \mathbf{x}') &= 2 \left(\sqrt{\frac{2}{m}} \sum_{k=0}^{\infty} (N\mu_{1,k} + \mu_{2,k}) F(d, k) G_k^{(\frac{d-1}{2})}(\langle \mathbf{x}, \mathbf{x}' \rangle) \right) \\ &\quad \cdot \left(\sqrt{\frac{2}{m}} \left(\sum_{k=0}^{\infty} \mu_{2,k} F(d, k) G_k^{(\frac{d-1}{2})}(\langle \mathbf{x}, \mathbf{x}' \rangle) \right) \right)^{N-1}\end{aligned}\tag{60}$$

Comparing the above equation with Eq. (5), it turns out that we need to simplify Eq. (60) and equate the polynomial coefficients on both equations. It is obvious that we get the form of the product of multiple polynomials in Eq. (60). Fortunately, the following Lemma allows us to express the product of two Gegenbauer polynomials as a linear combination of other Gegenbauer polynomials.

Lemma 8. [Carlitz, 1961, Eq (8)] For $b \in \mathbb{R}$ and any $p, q \in \mathbb{N}$, there exists a set of positive coefficients $\{\lambda_s^{(p,q)}\}_{s=0}^{\min(p,q)}$ such that

$$G_p^{(b)}(x) G_q^{(b)}(x) = \sum_{s=0}^{\min(p,q)} \lambda_s^{(p,q)} G_{p+q-2s}^{(b)}(x),\tag{61}$$

where

$$\lambda_s^{(p,q)} = \frac{p+q+v-2s}{p+q+v-s} \cdot \frac{(v)_s (v)_{p-s} (v)_{q-s}}{s!(p-s)!(q-s)!} \cdot \frac{(2v)_{p+q-s}}{(v)_{p+q-s}} \cdot \frac{(p+q-2s)!}{(2v)_{p+q-2s}},$$

and

$$(v)_k := v(v+1)(v+2)\dots(v+k-1), \quad (v)_0 := 1.$$

For convenience, we assume v is an integer and k even, then we set $p = q = k$, $s = 0$, and apply Lemma 8 recursively by N times, we can obtain the lower bound regarding the coefficient of the term $C_{Nk}^{(\frac{d-1}{2})}$, which is the (Nk) th harmonic:

$$\mu_{Nk} F(d, Nk) \geq \left(\sqrt{\frac{2}{m}} F(d, k) \right)^N (N\mu_{1,k} + \mu_{2,k}) \mu_{2,k}^{N-1} \prod_{\alpha=1}^N \lambda_0^{(k, \alpha k)}.\tag{62}$$

It suffices to obtain the form of $\lambda_0^{(k, \alpha k)}$. The coefficient $\lambda_0^{(k, \alpha k)}$ defined in Lemma 8

$$\begin{aligned}\lambda_0^{(k, \alpha k)} &= \frac{(\alpha k + k) + v}{(\alpha k + k) + v} \cdot \frac{(v)_0 (v)_k (v)_{\alpha k}}{0!(k)!(\alpha k)!} \cdot \frac{(2v)_{(\alpha k + k)}}{(v)_{(\alpha k + k)}} \cdot \frac{(\alpha k + k)!}{(2v)_{(\alpha k + k)}} \\ &= \frac{(v)_k (v)_{\alpha k}}{(k)!(\alpha k)!} \cdot \frac{(\alpha k + k)!}{(v)_{(\alpha k + k)}} \\ &= \frac{(v+k-1)!(v+\alpha k-1)!}{((v-1)!)^2 (k)!(\alpha k)!} \cdot \frac{(\alpha k + k)!(v-1)!}{(v+\alpha k+k-1)!} \\ &= \frac{(v+k-1)!(v+\alpha k-1)!}{(v-1)!(k)!(\alpha k)!} \cdot \frac{(\alpha k + k)!}{(v+\alpha k+k-1)!} \\ &\sim \frac{(v+k-1)^{(v+k-0.5)} (v+\alpha k-1)^{(v+\alpha k-0.5)}}{(v-1)^{(v-0.5)} k^{(k+0.5)} (\alpha k)^{(\alpha k+0.5)}} \cdot \frac{(\alpha k + k)^{(\alpha k+k+0.5)}}{(v+\alpha k+k-1)^{(v+\alpha k+k-0.5)}},\end{aligned}\tag{63}$$

where we apply the Stirling's approximation ($n! \sim \sqrt{2\pi n}(\frac{n}{e})^n$) at the final step. Next, we consider the case when $k \gg v$. In order to match the term $C_{Nk}^{(\frac{d-1}{2})}$ in Eq. (60), we set $v = (d-1)/2$ and obtain:

$$\begin{aligned} \lambda_0^{(k, \alpha k)} &\sim \frac{(k)^{(v+k-0.5)}(\alpha k)^{(v+\alpha k-0.5)}}{k^{(k+0.5)}(\alpha k)^{(\alpha k+0.5)}} \cdot \frac{(\alpha k + k)^{(\alpha k + k + 0.5)}}{(\alpha k + k)^{(v+\alpha k + k - 0.5)}} \\ &\sim (k)^{(v-1)}(\alpha k)^{(v-1)}(\alpha k + k)^{(-v-1)} \sim \left(\frac{\alpha k}{1+\alpha}\right)^{v-1} = \left(\frac{\alpha k}{1+\alpha}\right)^{\frac{d-3}{2}}. \end{aligned} \quad (64)$$

Plugging Eq. (64) into Eq. (62), we obtain:

$$\begin{aligned} \mu_{Nk} &\geq \frac{\left(\sqrt{\frac{2}{m}}F(d, k)\right)^N}{F(d, Nk)} (N\mu_{1,k} + \mu_{2,k})\mu_{2,k}^{N-1} \prod_{\alpha=1}^N \lambda_0^{(k, \alpha k)} \\ &\sim \frac{F(d, k)^N}{F(d, Nk)} (N\mu_{1,k} + \mu_{2,k})\mu_{2,k}^{N-1} \left(\frac{k}{N}\right)^{\frac{d-3}{2}} \\ &\sim \frac{k^{Nd}}{(Nk)^d} (N\mu_{1,k} + \mu_{2,k})\mu_{2,k}^{N-1} \left(\frac{k}{N}\right)^{\frac{d-3}{2}} \quad (\text{by Stirling}) \\ &\sim \frac{k^{Nd}}{(Nk)^d} \Omega(k^{-Nd-N}) \left(\frac{k}{N}\right)^{\frac{d-3}{2}} \\ &\sim \Omega((kN^3)^{-\frac{d}{2}}) \end{aligned} \quad (65)$$

Setting $k = k'/N$ allows us to conclude the proof. \square

E Details on the numerical experiments

In the following content, we will describe the setup of several experiments including learning analytically-known function (Appendix E.1), variation of darkness (Appendix E.2), arithmetic extrapolation (Appendix E.3), and learning harmonics (Appendix E.4). The experiment of visual analogy task is included in Appendix E.5. The experiment on the spectral bias in image classification is contained in Appendix E.6

E.1 Experimental setup in learning analytically-known function

We describe the experimental setup corresponding to Section 4.1. N -layer fully-connected NNs are compared against NNs-Hp with $N-1$ degree multiplicative interactions. The reason is that one-degree PNNs are equivalent to two-layer fully-connected NNs, according to the formula of PNNs provided in Eq. (1). In the experiment, the training set consists of 20000 data points in total. The networks are trained for 50 epochs with batch size 256. The squared loss is minimized through ADAM optimizer [Kingma and Ba, 2015] with $\beta_1 = 0.9$, $\beta_2 = 0.999$, learning rate = 10^{-4} .

As a complement, we show additional results of fitting two-variable functions in Figure 6 to further examine the power of Hadamard product.

In our work, the extrapolation relies on the support of the training data [van Schuppen, 2021], as suggested by the previous work of Xu et al. [2021]. We note that for certain applications and input data types, the convex hull might be required, however, we leave this as future work.

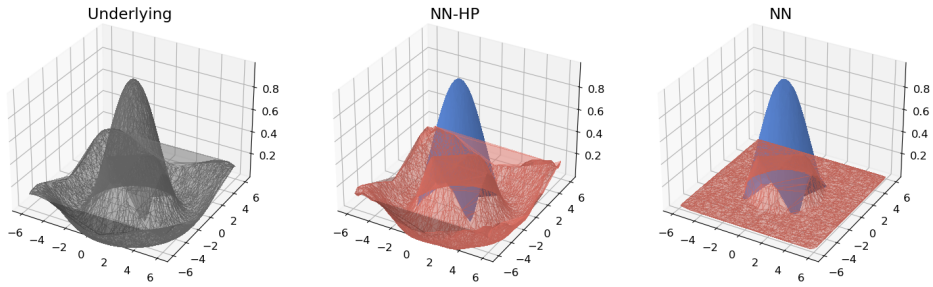
E.2 Experimental setup in variation of darkness

This section describes the experimental setup of the variation of darkness experiment in Section 4.2. The following two datasets are used: (a) MNIST dataset [LeCun et al., 1998], which contains handwritten digits images from zero to nine. There are 60,000 examples in the training set and

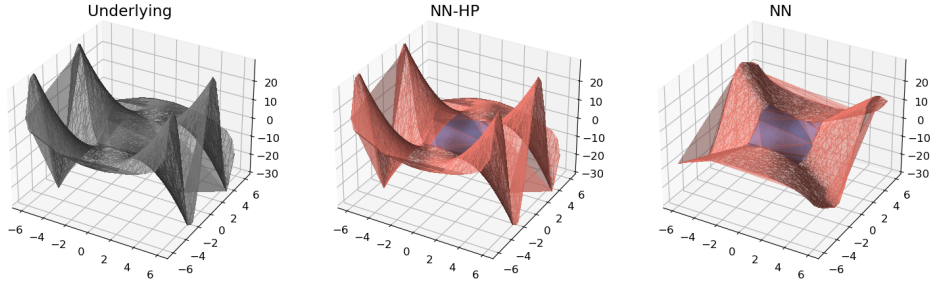
10,000 examples in the testing set. Each image has the resolution 28×28 . (b) Fashion-MNIST dataset [Xiao et al., 2017], which contains images of clothing with 10 classes. There are 60,000 examples in the training set and 10,000 examples in the testing set. Each image has the resolution 28×28 . The networks are trained for 20 epochs with batch size 128 with the criterion of cross entropy loss. The learning rate is chosen as 0.01. The width of the networks is 256. Each network is trained for 3 runs.

E.3 Experimental setup in arithmetic extrapolation

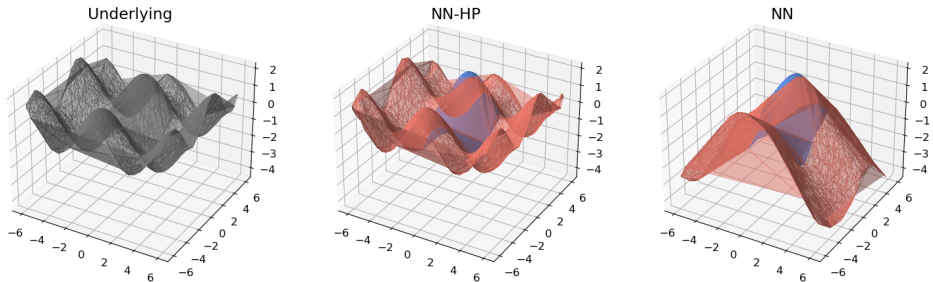
This section describes the experimental setup of the arithmetic extrapolation experiment in Section 4.2. We construct a new dataset based on the MNIST dataset [LeCun et al., 1998] to demonstrate the addition of two (visual) numbers. We randomly pick 90 combinations of two digits for training (out of the 100 total combinations), and then we use the rest 10 for extrapolation set. Specifically, in our three-fold cross-validation, we randomly pick up 90 combinations of two digits and we sample 2000



(a) Fitting results for underlying function $f_{\rho}(\mathbf{x}) = \frac{\sin(\sqrt{\|\mathbf{x}\|_2})}{\sqrt{\|\mathbf{x}\|_2}}$, where $\|\cdot\|_2$ indicates the Euclidean norm. The prediction within the training (extrapolation) region is presented by blue (red) color.



(b) Fitting results for underlying function $f_{\rho}(\mathbf{x}) = (x^{(1)})^2 \times \sin(x^{(2)})$. The prediction within the training (extrapolation) region is presented by blue (red) color.



(c) Fitting results for the underlying function $f_{\rho}(\mathbf{x}) = \cos(x^{(1)}) + \sin(x^{(2)})$. The prediction within the training (extrapolation) region is presented by blue (red) color.

Figure 6: This figure shows the results of fitting several analytically-known two-variable functions. We can see even though both NNs-Hp and NNs can learn well in the training region, NNs-Hp is much more flexible than standard NNs during extrapolation.

pairs for each combination to construct the training set. There are 90×2000 pairs in the training set and 10×2000 pairs in the testing set. Each network is trained for 100 epochs with batch size 128. The width of the networks is 256. Each network is trained with squared-loss for 3 runs.

E.4 Experimental setup in learning harmonics

This section describes the experimental setup corresponding to Section 4.3. We follow the setup in Cao et al. [2019], Choraria et al. [2022]. The number of sample points is 1000. The width of the network is 32768. The network is trained for 30000 iterations and optimized via stochastic gradient descent with learning rate 0.0016.

E.5 Visual analogy task

In this section, we scrutinize the extrapolation capability of NNs-Hp on the visual analogy task on VAEC dataset Webb et al. [2020]. For each pair of four images A, B, C, D , the proportional analogy problem is in the form $A : B :: C : D$ based on the brightness, size, and 2-D location. The model is required to select the correct D among several candidates when given A, B, C . We conduct the scale extrapolation experiment introduced in the paper as it’s similar to our experiment on the variation of brightness, which treats the scale factor α as the extent of extrapolation. $\alpha = 1$ indicates the training set. $\alpha \in \{2, \dots, 6\}$ indicates the extrapolation set, where the values of the dataset are multiplied by a scale factor α ranging from 2 to 6. We use the original best model in the paper as baseline (NNs) and insert Hadamard product as NNs-Hp to compare. Apart from the network architecture, the training details are the same as in Webb et al. [2020]. We run each method 8 times and report the mean of accuracy in Table 3. Results show that both models achieve similar performance in the training regime while NNs-HP extrapolates better than standard NNs in most regimes.

Table 3: Experimental results in the task of visual analogy on VAEC dataset. ‘Ext’ abbreviates ‘extrapolation’. We can see that NNs-HP has better extrapolation performance in most extrapolation regimes.

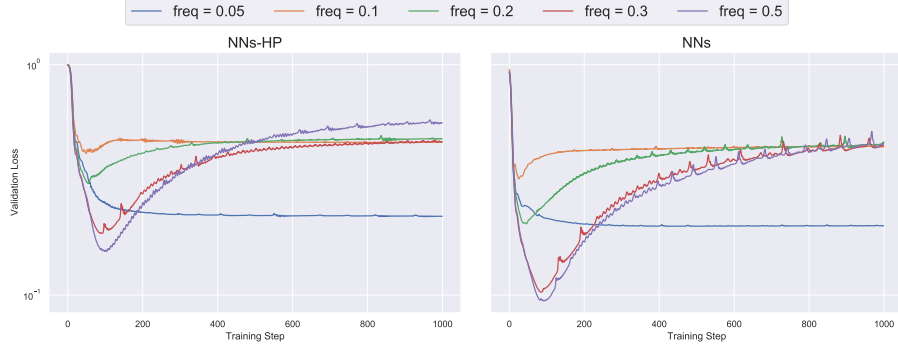
	Training ($\alpha = 1$)	Ext ($\alpha = 2$)	Ext ($\alpha = 3$)	Ext ($\alpha = 4$)	Ext ($\alpha = 5$)	Ext ($\alpha = 6$)
NNs	99.5%	76.2%	55.5%	46.3%	42.6%	40.4%
NNs-Hp	99.7%	73.7%	57.5%	49.0%	45.3%	42.9%

E.6 Spectral bias in image classification

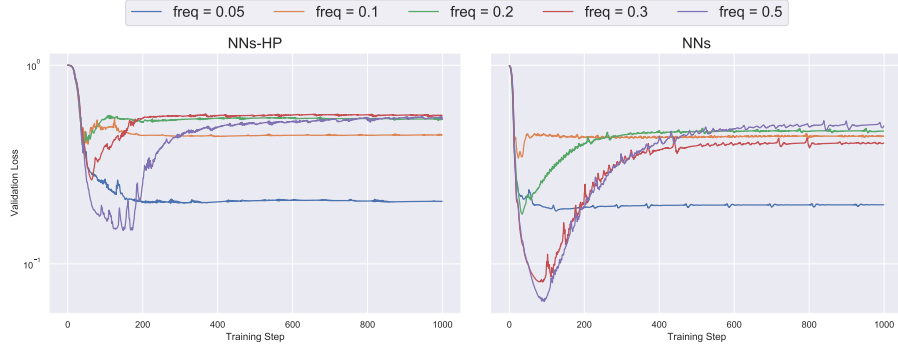
This experiment studies how the frequency of the noise affects the validation performance in image classification, which further validates our theoretical result on spectral bias in Section 3.3. Specifically, we follow the standard set up in Rahaman et al. [2019]. we consider a binary classification task with labels 3 and 8 on the MNIST dataset. We add noises with different frequencies to the label. We test NNs-Hp with three, six, and nine-degree multiplicative interaction and compare it with the corresponding standard fully-connected neural networks. Both networks are optimized through Adam. We select mean squared loss as the criterion and choose learning rate 0.0001. We train each network for 1000 iterations. The width of the network is 256. The results in Figure 7 present the ‘dip’ of validation mean squared error (MSE) during the process of training. In the comparison of each order, for instance, in Figure 7a we can see that in the case of higher frequencies, e.g., 0.3 and 0.5, the validation dips of NNs-Hp are apparently smaller than that of NNs in the early stage of during training. The reason is that NNs-Hp can speed up the learning of high-frequency information based on Section 3.3.

F Additional result on multiplicative filter networks

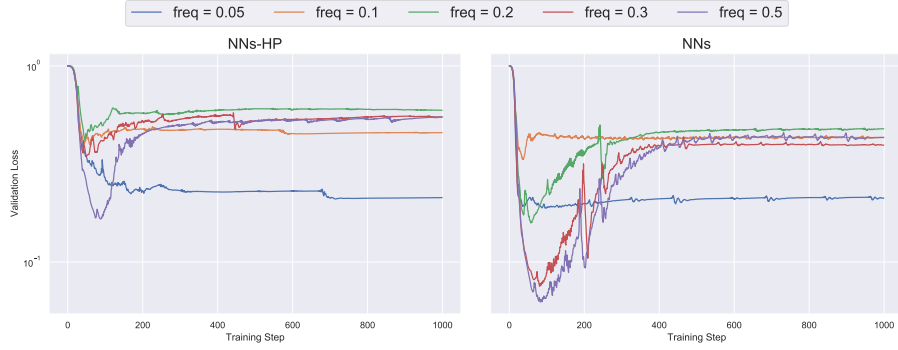
Multiplicative filter network (MFN) is another instance of NNs-Hp which inserts the Hadamard between the sinusoidal or Gabor wavelet functions among each layer [Fathony et al., 2021]. MFN has demonstrated stronger performance over standard neural networks in several representation tasks.



(a) Results of NNs-Hp with three-degree multiplicative interaction and the corresponding NNs.



(b) Results of NNs-Hp with six-degree multiplicative interaction and the corresponding NNs.



(c) Results of NNs-Hp with nine-degree multiplicative interaction and the corresponding NNs.

Figure 7: The above figures show the dip of validation loss of NNs-Hp and NNs during training. Since NNs-Hp is able to speed up learning high-frequency information, we can see that for high-frequency noise, such dip for NNs-Hp is smaller than that of NNs at the early stage of training.

F.1 Theoretical analysis

In this section, we will derive the neural tangent kernel of MFN and then analyze the extrapolation behavior of MFN. We consider the following MFN:

$$\mathbf{y}_1 = \sqrt{\frac{2}{m}} \sin(\mathbf{W}_1 \mathbf{x}), \quad f(\mathbf{x}) = \sqrt{\frac{2}{m}} (\mathbf{W}_{N+1} \mathbf{y}_N), \quad \mathbf{y}_n = \sqrt{\frac{2}{m}} \sin(\mathbf{W}_n \mathbf{x}) * \mathbf{y}_n, \quad n = 2, \dots, N,$$

where each element in $\mathbf{W}_{N+1} \in \mathbb{R}^{1 \times m}$ and $\mathbf{W}_n \in \mathbb{R}^{m \times d}$, for $n = 1, \dots, N$ is independently sampled from $\mathcal{N}(0, 1)$. Note that we multiply by the scaling factor $\sqrt{\frac{2}{m}}$ after each degree to ensure that the norm of the network output is preserved at initialization with infinite-width setting. In Lemma 9 we develop the NTK $K(\mathbf{x}, \mathbf{x}')$ of MFN.

Lemma 9. *The neural tangent kernel of the MFN has the following form:*

$$K(\mathbf{x}, \mathbf{x}') = 2N \cdot \langle \mathbf{x}, \mathbf{x}' \rangle \kappa_3(\mathbf{x}, \mathbf{x}') (\kappa_4(\mathbf{x}, \mathbf{x}'))^{N-1} + 2(\kappa_4(\mathbf{x}, \mathbf{x}'))^N, \quad (66)$$

where κ_3 and κ_4 are defined by taking the random Gaussian vector $\mathbf{w} \in \mathbb{R}^d$,

$$\kappa_3 = \mathbb{E}_{\mathbf{w} \sim \mathcal{N}(\mathbf{0}, \frac{2}{m} \cdot \mathbf{I})} (\cos(\mathbf{w}^\top \mathbf{x}) \cdot \cos(\mathbf{w}^\top \mathbf{x}')), \quad \kappa_4 = \mathbb{E}_{\mathbf{w} \sim \mathcal{N}(\mathbf{0}, \frac{2}{m} \cdot \mathbf{I})} (\sin(\mathbf{w}^\top \mathbf{x}) \cdot \sin(\mathbf{w}^\top \mathbf{x}')).$$

Proof of Lemma 9. We will compute the gradient with respect to each weight and then sum up the inner products to obtain the NTK. Below, we denote by $\tilde{\alpha}_n = \mathbf{W}_n \mathbf{x}, n \in [N]$. Firstly, we compute the contribution to the NTK w.r.t \mathbf{W}_1 , its corresponding derivative is as follows:

$$\begin{aligned} \partial_{\mathbf{W}_1} f(\mathbf{x}) &= \sqrt{\frac{2}{m}} \left[\mathbf{W}_{N+1}^\top \left(\prod_{n=2}^N \text{Diag} \left(\sin \left(\sqrt{\frac{2}{m}} \tilde{\alpha}_n(\mathbf{x}) \right) \right) \right) \cos \left(\sqrt{\frac{2}{m}} \tilde{\alpha}_1(\mathbf{x}) \right) \right]^\top (\partial_{\mathbf{W}_1} \tilde{\alpha}_1(\mathbf{x}))^\top \\ &= \sqrt{\frac{2}{m}} \left[\mathbf{W}_{N+1}^\top \left(\prod_{n=2}^N \text{Diag} \left(\sin \left(\sqrt{\frac{2}{m}} \tilde{\alpha}_n(\mathbf{x}) \right) \right) \right) \cos \left(\sqrt{\frac{2}{m}} \tilde{\alpha}_1(\mathbf{x}) \right) \right]^\top \mathbf{x}^\top \end{aligned}$$

where $\text{Diag}(\cdot)$ converts a vector to a diagonal matrix. The inner product follows that:

$$\begin{aligned} &\langle \partial_{\mathbf{W}_1} f(\mathbf{x}), \partial_{\mathbf{W}_1} f(\mathbf{x}') \rangle \\ &= \frac{2}{m} \sum_{j=1}^m W_{N+1}^{(j)} W_{N+1}^{(j)} \left(\prod_{n=2}^N \left(\frac{2}{m} \sin(\tilde{\alpha}_n^{(j)}(\mathbf{x})) \sin(\tilde{\alpha}_n^{(j)}(\mathbf{x}')) \right) \right) \left(\frac{2}{m} \cos(\tilde{\alpha}_1^{(j)}(\mathbf{x})) \cos(\tilde{\alpha}_1^{(j)}(\mathbf{x}')) \right) \mathbf{x}^\top \mathbf{x}'. \end{aligned} \quad (67)$$

By the law of large numbers, we obtain:

$$\lim_{m \rightarrow \infty} \langle \partial_{\mathbf{W}_1} f(\mathbf{x}), \partial_{\mathbf{W}_1} f(\mathbf{x}') \rangle = 2 \langle \mathbf{x}, \mathbf{x}' \rangle \kappa_3(\mathbf{x}, \mathbf{x}') (\kappa_4(\mathbf{x}, \mathbf{x}'))^{N-1}. \quad (68)$$

Since the formula of the network is symmetric w.r.t $\{\mathbf{W}_i\}_{i=1}^N$, the contributions of $\{\mathbf{W}_i\}_{i=1}^N$ to the NTK are the same, we can trivially multiply Eq. (68) by N .

Next, we will compute the contribution to the NTK w.r.t \mathbf{W}_{N+1} , its corresponding derivative is as follows:

$$\partial_{\mathbf{W}_{N+1}} f(\mathbf{x}) = \sqrt{\frac{2}{m}} \left(\sqrt{\frac{2}{m}} \sin(\tilde{\alpha}_N) * \dots * \sqrt{\frac{2}{m}} \sin(\tilde{\alpha}_1) \right).$$

The inner product follows that:

$$\langle \partial_{\mathbf{W}_{N+1}} f(\mathbf{x}), \partial_{\mathbf{W}_{N+1}} f(\mathbf{x}') \rangle = \frac{2}{m} \sum_{j=1}^m \left(\prod_{n=1}^N \left(\frac{2}{m} \sin(\tilde{\alpha}_n^{(j)}(\mathbf{x})) \sin(\tilde{\alpha}_n^{(j)}(\mathbf{x}')) \right) \right).$$

By the law of large numbers:

$$\begin{aligned} &\lim_{m \rightarrow \infty} \langle \partial_{\mathbf{W}_{N+1}} f(\mathbf{x}), \partial_{\mathbf{W}_{N+1}} f(\mathbf{x}') \rangle \\ &= 2 \cdot (\kappa_4(\mathbf{x}, \mathbf{x}'))^N. \end{aligned} \quad (69)$$

The proof is completed by multiplying Eq. (68) by N and adding by Eq. (69). \square

The derived kernel enables us to study how MFN trained by gradient descent extrapolates.

Theorem 8. *Suppose we train MFN with N -degree multiplicative interaction with infinite-width on $\{(\mathbf{x}_i, y_i)\}_{i=1}^{|\mathcal{X}|}$, and the network is optimized with squared loss in the NTK regime. For any direction $\mathbf{v} \in \mathbb{R}^d$ that satisfies $\|\mathbf{v}\|_2 = \max\{\|\mathbf{x}_i\|_2\}$, let $\mathbf{x}_0 = t\mathbf{v}$ and $\mathbf{x} = \mathbf{x}_0 + h\mathbf{v}$ with $t > 1$ and $h > 0$ be the extrapolation data points, the output $f(\mathbf{x}_0 + h\mathbf{v})$ can extrapolate to $\text{poly} = (\sin(\alpha t), \cos(\alpha t), t)$, where α is constant and the order of $\sin(\alpha t)$ is up to N , the order of $\cos(\alpha t)$ and t is one.*

Proof of Theorem 8. A specific feature map $\phi(\mathbf{x})$ induced by the NTK of MFN is

$$\phi(\mathbf{x}) = (c' \mathbf{x} \cdot \cos\langle \mathbf{w}, \mathbf{x} \rangle \cdot \sin(\langle \mathbf{w}, \mathbf{x} \rangle)^{N-1}, c'' \sin(\langle \mathbf{w}, \mathbf{x} \rangle)^N), \quad (70)$$

where \mathbf{w} is sampled from $\mathcal{N}(\mathbf{0}, \mathbf{I})$, c' and c'' are constants. Note that kernel regression solution is equivalent to the following form:

$$f(\mathbf{x}) = \boldsymbol{\beta}^\top \phi(\mathbf{x}), \quad (71)$$

where the representation coefficient $\boldsymbol{\beta}$ holds:

$$\begin{aligned} & \min_{\boldsymbol{\beta}'} \|\boldsymbol{\beta}'\|_2 \\ & \text{s.t. } \phi(\mathbf{x}_i)^\top \boldsymbol{\beta}' = y_i, \quad i = 1, \dots, |\mathcal{X}|. \end{aligned} \quad (72)$$

Therefore, given inputs $\mathbf{x}_0 = t\mathbf{v}$ and $\mathbf{x} = \mathbf{x}_0 + h\mathbf{v}$, we have:

$$\begin{aligned} f(\mathbf{x}) - f(\mathbf{x}_0) &= \boldsymbol{\beta}^\top (\phi((t+h)\mathbf{v}) - \phi(t\mathbf{v})) \\ &= \beta_1^\top (c'(t+h)\mathbf{v} \cdot \cos\langle \mathbf{w}, (t+h)\mathbf{v} \rangle \cdot \sin(\langle \mathbf{w}, (t+h)\mathbf{v} \rangle)^{N-1}) \\ &\quad - \beta_1^\top (c't\mathbf{v} \cdot \cos\langle \mathbf{w}, t\mathbf{v} \rangle \cdot \sin(\langle \mathbf{w}, t\mathbf{v} \rangle)^{N-1}) \\ &\quad + \beta_2 (c'' \sin(\langle \mathbf{w}, (t+h)\mathbf{v} \rangle)^N) - \beta_2 (c'' \sin(\langle \mathbf{w}, t\mathbf{v} \rangle)^N), \end{aligned}$$

Therefore, the network can extrapolate to poly = $(\sin(\alpha t), \cos(\alpha t), t)$, where α is constant and the order of $\sin(\alpha t)$ is up to N . This completes the proof. \square

E.2 Numerical result

In this section, we provide additional experimental results on extrapolation with MFN. Firstly, we follow the setup in Appendix E.5 and present the result on VAEC dataset as follows, where we can see that We can see that MFN has better extrapolation performance than standard NN in most extrapolation regimes.

Table 4: Experimental results in the task of visual analogy on VAEC dataset. 'Ext' abbreviates 'extrapolation'.

	Training ($\alpha = 1$)	Ext ($\alpha = 2$)	Ext ($\alpha = 3$)	Ext ($\alpha = 4$)	Ext ($\alpha = 5$)	Ext ($\alpha = 6$)
NN	99.5%	76.2%	55.5%	46.3%	42.6%	40.4%
MFN	99.1%	74.5%	56.2%	47.1%	43.0%	40.6%

Next, we apply MFN in the task of arithmetic extrapolation, as introduced in Section 4.2, and follow the same experimental setup. The following result further showcases the improvement of MFN over standard NN.

Table 5: Results with MFN and standard NN in the task of arithmetic extrapolation.

Method		Rounding	Floor/ceiling	± 1
NN(Dense)	Interpolation	0.980	0.999	0.999
	Extrapolation	0.436	0.805	0.887
MFN (Dense)	Interpolation	0.996	0.997	0.999
	Extrapolation	0.720	0.874	0.916
NN(Conv)	Interpolation	0.945	0.983	0.994
	Extrapolation	0.617	0.918	0.953
MFN (Conv)	Interpolation	0.947	0.996	0.999
	Extrapolation	0.824	0.925	0.954

G Additional result on non-local networks with Hadamard product

Non-local networks have demonstrated stellar performance in capturing long-range dependencies of the input signals [Wang et al., 2018]. Particularly, Poly-NL is one of the non-local networks that

utilize three-degree polynomial to reduce the complexity of traditional non-local networks from quadratic to linear. Note that the formula in [Babiloni et al., 2021] is based on standard polynomial expansion, which we have analyzed in the main body. To make our analysis more general, we consider the following single Poly-NL block that uses Softmax as activation function:

$$\begin{aligned} \mathbf{y}_1 &= \mathbf{x}, \quad \mathbf{y}_2 = \sigma(\mathbf{W}_1 \mathbf{y}_1), \\ \mathbf{y}_3 &= \text{Softmax}\{(\mathbf{w}_Q \mathbf{y}_2^\top) * (\mathbf{w}_K \mathbf{y}_2^\top)\} (\mathbf{y}_2 w_V), \\ f(\mathbf{x}) &= \sqrt{\frac{2}{m}} (\mathbf{w}_2^\top \mathbf{y}_3), \end{aligned}$$

where $\mathbf{x} \in \mathbb{R}^d$, $\mathbf{W}_1 \in \mathbb{R}^{m \times d}$, $\mathbf{w}_Q \in \mathbb{R}^m$, $\mathbf{w}_K \in \mathbb{R}^m$, $w_V \in \mathbb{R}$, $\mathbf{w}_2 \in \mathbb{R}^m$, each element in the weight is independently sampled from $\mathcal{N}(0, 1)$, the Softmax is row-wise. Firstly, we give the neural tangent kernel of the Poly-NL, wherein we only train the weight w_Q and w_K .

Lemma 10. *The neural tangent kernel of the Poly-NL has the following form:*

$$K(\mathbf{x}, \mathbf{x}') = 4 \cdot \mathbb{E}_{w_3, w_4 \sim \mathcal{N}(0, 1)} \mathbf{y}_2^\top (\text{Diag}(\boldsymbol{\tau}) - \boldsymbol{\tau} \boldsymbol{\tau}^\top) (\mathbf{y}_2 * \mathbf{y}_2) \mathbf{y}_2'^\top (\text{Diag}(\boldsymbol{\tau}') - \boldsymbol{\tau}' \boldsymbol{\tau}'^\top) (\mathbf{y}_2' * \mathbf{y}_2'),$$

where we denote by $\boldsymbol{\tau} = \text{Softmax}(w_3 w_4 (\mathbf{y}_2 * \mathbf{y}_2))$, $\boldsymbol{\tau}' = \text{Softmax}(w_3 w_4 (\mathbf{y}_2' * \mathbf{y}_2'))$, $\mathbf{y}_2 = \sigma(\mathbf{W}_1 \mathbf{x})$, $\mathbf{y}_2' = \sigma(\mathbf{W}_1 \mathbf{x}')$, where w_3 and w_4 is independently sampled from $\mathcal{N}(0, 1)$.

Proof of Lemma 10. Firstly, we compute the Jacobian with respect to w_Q :

$$\begin{aligned} \partial_{w_Q} f(\mathbf{x}) &= \sqrt{\frac{2}{m}} \frac{\partial \left(\sum_{i=1}^m w_2^{(i)} y_3^{(i)} \right)}{\partial w_Q} \\ &= \sqrt{\frac{2}{m}} \sum_{i=1}^m w_2^{(i)} w_V \mathbf{y}_2^\top \frac{\partial \text{Softmax} \left(w_Q^{(i)} w_K^{(i)} (\mathbf{y}_2 * \mathbf{y}_2) \right)}{\partial w_Q} \\ &= \sqrt{\frac{2}{m}} \sum_{i=1}^m w_2^{(i)} w_K^{(i)} w_V \mathbf{y}_2^\top (\text{Diag}(\boldsymbol{\varphi}_i) - \boldsymbol{\varphi}_i \boldsymbol{\varphi}_i^\top) (\mathbf{y}_2 * \mathbf{y}_2) \mathbf{e}_i^\top, \end{aligned}$$

where we denote by $\boldsymbol{\varphi}_i = \text{Softmax} \left(w_Q^{(i)} w_K^{(i)} (\mathbf{y}_2 * \mathbf{y}_2) \right) \in \mathbb{R}^m$. Next, in order to obtain the NTK, we calculate the inner product of the Jacobian:

$$\begin{aligned} &\langle \partial_{w_Q} f(\mathbf{x}), \partial_{w_Q} f(\mathbf{x}') \rangle \\ &= \frac{2}{m} \sum_{i=1}^m (w_2^{(i)} w_K^{(i)} w_V)^2 \mathbf{y}_2^\top (\text{Diag}(\boldsymbol{\varphi}_i) - \boldsymbol{\varphi}_i \boldsymbol{\varphi}_i^\top) (\mathbf{y}_2 * \mathbf{y}_2) \mathbf{y}_2'^\top (\text{Diag}(\boldsymbol{\varphi}'^i) - \boldsymbol{\varphi}'^i \boldsymbol{\varphi}'^{i\top}) (\mathbf{y}_2' * \mathbf{y}_2') \end{aligned}$$

By the law of large numbers, as $m \rightarrow \infty$, we obtain:

$$\begin{aligned} &\lim_{m \rightarrow \infty} \langle \partial_{w_Q} f(\mathbf{x}), \partial_{w_Q} f(\mathbf{x}') \rangle \\ &= 2 \cdot \mathbb{E}_{w_3, w_4 \sim \mathcal{N}(0, 1)} \mathbf{y}_2^\top (\text{Diag}(\boldsymbol{\tau}) - \boldsymbol{\tau} \boldsymbol{\tau}^\top) (\mathbf{y}_2 * \mathbf{y}_2) \mathbf{y}_2'^\top (\text{Diag}(\boldsymbol{\tau}') - \boldsymbol{\tau}' \boldsymbol{\tau}'^\top) (\mathbf{y}_2' * \mathbf{y}_2'), \quad (73) \end{aligned}$$

where we denote by $\boldsymbol{\tau} = \text{Softmax}(w_3 w_4 (\mathbf{y}_2 * \mathbf{y}_2))$. Since the weight w_Q and w_K are symmetric in the formula of Poly-NL, the proof is completed by multiplying Eq. (73) by two. \square

Now we are ready to analyze the extrapolation behaviour of Poly-NL.

Theorem 9. *Suppose we train Poly-NL with infinite-width on $\{(\mathbf{x}_i, y_i)\}_{i=1}^{|\mathcal{X}|}$, and the network is optimized with squared loss in the NTK regime. For any direction $\mathbf{v} \in \mathbb{R}^d$ that satisfies $\|\mathbf{v}\|_2 = \max\{\|\mathbf{x}_i\|_2^2\}$, let $\mathbf{x}' = t\mathbf{v}$ and $\mathbf{x} = \mathbf{x}' + h\mathbf{v}$ with $t > 1$ and $h > 0$ be the extrapolation data points, then for $\delta \in (0, 1)$ and some constant C , when $m \geq 2 \ln(2/\delta) + d + \sqrt{8d \ln(2/\delta)}$, with probability at least $1 - \delta$, we have:*

$$|f(\mathbf{x}) - f(\mathbf{x}')| \leq Ct^3 h^3 m^{\frac{3}{2}} \|\mathbf{v}\|^3.$$

Proof of Theorem 9. We first bound the spectral norm of the weight matrix \mathbf{W}_1 .

Lemma 11. *Based on the randomness of the weight \mathbf{W}_1 , for $\delta \in (0, 1)$, when $m \geq 2 \ln(2/\delta) + d + \sqrt{8d \ln(2/\delta)}$, with probability at least $1 - \delta$, we have $\|\mathbf{W}_1\| \leq 2\sqrt{m}$.*

We can choose a certain feature map $\phi(\mathbf{x})$ induced by the NTK in Lemma 10 is

$$\phi(\mathbf{x}) = (\mathbf{y}_2^\top (\text{Diag}(\boldsymbol{\tau}) - \boldsymbol{\tau}\boldsymbol{\tau}^\top) (\mathbf{y}_2 * \mathbf{y}_2)) , \quad (74)$$

where $\tilde{\boldsymbol{\tau}} = \text{Softmax}(w_5 w_6 (\mathbf{y}_2 * \mathbf{y}_2))$, w_5, w_6 are iid sampled from $\mathcal{N}(0, 1)$, c' and c'' are constants. Similarly, using the solution of kernel regression, we can calculate the output of the network as follows. Given $\mathbf{x}' = t\mathbf{v}$ and $\mathbf{x} = \mathbf{x}' + h\mathbf{v}$, we add the prime symbol to the variable in the network associated to the input \mathbf{x}' , we have:

$$\begin{aligned} |f(\mathbf{x}) - f(\mathbf{x}')| &= |\beta (\phi((t+h)\mathbf{v}) - \phi(t\mathbf{v}))| \\ &\leq |\beta| \|\mathbf{y}_2\| \|\text{Diag}(\boldsymbol{\tau}) - \boldsymbol{\tau}\boldsymbol{\tau}^\top\| \|\mathbf{y}_2 * \mathbf{y}_2 - \mathbf{y}'_2 * \mathbf{y}'_2\| \\ &\quad + |\beta| \|\mathbf{y}'_2 * \mathbf{y}'_2\| \|\mathbf{y}_2\| \|\text{Diag}(\boldsymbol{\tau}) - \boldsymbol{\tau}\boldsymbol{\tau}^\top - (\text{Diag}(\boldsymbol{\tau}') - \boldsymbol{\tau}'\boldsymbol{\tau}'^\top)\| \\ &\quad + |\beta| \|\mathbf{y}'_2 * \mathbf{y}'_2\| \|\text{Diag}(\boldsymbol{\tau}') - \boldsymbol{\tau}'\boldsymbol{\tau}'^\top\| \|\mathbf{y}_2 - \mathbf{y}'_2\|. \end{aligned} \quad (75)$$

We start by bounding the first term in Eq. (75). For $\delta \in (0, 1)$, when $m \geq 2 \ln(2/\delta) + d + \sqrt{8d \ln(2/\delta)}$, with probability at least $1 - \delta$, we have:

$$\begin{aligned} &|\beta| \|\mathbf{y}_2\| \|\text{Diag}(\boldsymbol{\tau}) - \boldsymbol{\tau}\boldsymbol{\tau}^\top\| \|\mathbf{y}_2 * \mathbf{y}_2 - \mathbf{y}'_2 * \mathbf{y}'_2\| \\ &\leq |\beta| \|\mathbf{y}_2\| (\|\text{Diag}(\boldsymbol{\tau})\| + \|\boldsymbol{\tau}\boldsymbol{\tau}^\top\|) (\|\mathbf{y}_2\| + \|\mathbf{y}'_2\|) (\|\mathbf{y}_2 - \mathbf{y}'_2\|) \\ &\leq 2|\beta| \|\mathbf{W}_1(t+h)\mathbf{v}\| (\|(t+h)\mathbf{W}_1\mathbf{v}\| + \|t\mathbf{W}_1\mathbf{v}\|) (\|h\mathbf{W}_1\mathbf{v}\|) \\ &\leq 4|\beta|(t+h)\sqrt{m}\|\mathbf{v}\| (2\sqrt{m}(t+h)\|\mathbf{v}\| + 2\sqrt{mt}\|\mathbf{v}\|) (2\sqrt{mh}\|\mathbf{v}\|) \\ &= 16|\beta|m^{\frac{3}{2}}\|\mathbf{v}\|^3 (2t^2h + 3th^2 + h^3). \end{aligned} \quad (76)$$

where the first inequality comes from triangle inequality, the second inequality is due to the fact that the output of softmax ranges from zero to one, and the 1-Lipschitz of ReLU. Next, we bound the second term in Eq. (75). Similarly, by Lemma 11, over the same randomness of the weight \mathbf{W}_1 , with probability at least $1 - \delta$, we have:

$$\begin{aligned} &|\beta| \|\mathbf{y}'_2 * \mathbf{y}'_2\| \|\mathbf{y}_2\| \|\text{Diag}(\boldsymbol{\tau}) - \boldsymbol{\tau}\boldsymbol{\tau}^\top - (\text{Diag}(\boldsymbol{\tau}') - \boldsymbol{\tau}'\boldsymbol{\tau}'^\top)\| \\ &\leq |\beta| \|\mathbf{y}'_2\|^2 \|\mathbf{y}_2\| (\|\text{Diag}(\boldsymbol{\tau} - \boldsymbol{\tau}')\| + \|\boldsymbol{\tau}\boldsymbol{\tau}^\top - \boldsymbol{\tau}'\boldsymbol{\tau}'^\top\|) \\ &\leq 4|\beta|mt^2\|\mathbf{v}\|^2 \times 2\sqrt{m}(t+h)\|\mathbf{v}\| \times 4 = 32|\beta|m^{\frac{3}{2}}\|\mathbf{v}\|^3(t^3 + t^2h). \end{aligned} \quad (77)$$

Next, we bound the third term in Eq. (75). Similarly, by Lemma 11, over the same randomness of the weight \mathbf{W}_1 , with probability at least $1 - \delta$, we have:

$$\begin{aligned} &|\beta| \|\mathbf{y}'_2 * \mathbf{y}'_2\| \|\text{Diag}(\boldsymbol{\tau}') - \boldsymbol{\tau}'\boldsymbol{\tau}'^\top\| \|\mathbf{y}_2 - \mathbf{y}'_2\| \\ &\leq |\beta| \|\mathbf{y}'_2\|^2 (\|\text{Diag}(\boldsymbol{\tau}')\| + \|\boldsymbol{\tau}'\boldsymbol{\tau}'^\top\|) \|\mathbf{y}_2 - \mathbf{y}'_2\| \\ &\leq 4mh^2|\beta|\|\mathbf{v}\|^2 \times 2 \times 2\sqrt{mh}\|\mathbf{v}\| = 16|\beta|m^{\frac{3}{2}}\|\mathbf{v}\|^3h^3. \end{aligned} \quad (78)$$

Therefore, the proof is completed by summing up Eq. (76) to (78). \square

H Societal impact

This work studies a cutting-edge network architecture, i.e., neural network with Hadamard product (NN-Hp), from a theoretical perspective. The analysis of the corresponding NTK lays a theoretical foundation for the interested practitioner to further study other priorities of NN-Hp such as convergence and generalization. Furthermore, our current analysis mainly focuses on the theoretical side of extrapolation. We believe our insight and empirical evidence in extrapolation will allow the investigation of other more complicated OOD problems among the ML community, such as domain adaption and invariant learning. Therefore, we do not expect any negative societal bias from this work.

I Limitations

In this work, we illustrate how our theory can be applicable in a variety of experimental settings, especially on extrapolation. Nevertheless, we do not focus explicitly on obtaining state-of-the-art numerical results in real-world applications, which could be one limitation of this work.

Our proof framework is based on NTK for understanding theoretical properties of neural networks. However, NTK still works in “linear” regime [Lee et al., 2019, Woodworth et al., 2020], which appears difficult to fully demonstrate the success of practical neural networks. Nevertheless, this is a common limitation of NTK-based analysis in the community.